

REAL-REFERENCE BUILDINGS FOR URBAN ENERGY MODELLING: A MULTISTAGE VALIDATION AND DIVERSIFICATION APPROACH

Ledesma, Gabriela^{a*}; Pons-Valladares, Oriol^a; Nikolic, Jelena^b

^a Department of Architectural Technology, School of Architecture (ETSAB), Universitat Politècnica de Catalunya (UPC-Barcelona Tech), Av. Diagonal 649, Barcelona 08028, Spain

^b Department of Physics, School of Architecture (ETSAB), Universitat Politècnica de Catalunya (UPC), Av. Diagonal 649, Barcelona 08028, Spain

*Corresponding author: maria.gabriela.ledesma@upc.edu

Abstract:

Urban energy models are required to establish baselines, map buildings' performance, and explore energy and CO₂ emissions reduction strategies. The authors propose a new reductive bottom-up model to estimate the final energy demand for educational building stocks. For this purpose, this model relies on data-driven validated real-reference buildings and probability up-scaling. This model has three stages: (1) multivariate clustering techniques identify real-reference buildings from building stocks, (2) calibrated energy simulation estimate demand, uncertainty and allow to test scenarios, and (3) probability up-scaling diversifies building-level results regarding variations in their urban emplacement. Afterwards, the authors applied this model to two educational building stocks: a conditioned stock in Barcelona, Spain and a free-floating stock in Quito, Ecuador. Two real-reference schools represent 62% of the stock in Barcelona, with a final energy demand of 15.96 GWh/year. Likewise, two schools describe the entire educational stock in Quito with a final energy demand of 29.83 GWh/year. Results reflect Barcelona stock is more heterogeneous than Quito despite its lesser population. Specifically, their energy use intensity was 85.92 kWh/m² with a 4.25% deviation in Barcelona and 40.23 kWh/m² with a 0.11% deviation in Quito. This model is transferable among stocks because it relies on the characterization of buildings' thermal balance in their as-is state and provides good accuracy with building and urban energy records. This diversification procedure gave back part of the lost variability because of the reductive approach in the real-reference building definition. Also, it produced lower prediction errors for aggregated final energy use.

Keywords:

Bottom-up model, energy use intensity, educational building stocks, probability up-scaling, archetype, data impact assessment

1. Introduction:

Analysts expect around 75 to 90% of the existing building stock to be functional by 2050 [1]. Two-thirds of this stock preceded energy efficiency legislation [2]. Hence, the current building stock is highly energy-intensive and contributes to the building sector responsibility for a third

of global primary energy use and greenhouse gas emissions [3]. Thus, it has an untapped potential for energy reduction in which small energy savings at the building level can cause significant savings at an urban scale. For this purpose, planners require identifying adequate replicable renovation strategies. Urban energy models (UEM) are efficient tools to describe and quantify building stocks and aid policy decision-making. Abundant UEMs are available in scientific literature and vary in their techniques, disaggregation level, data sources, assumptions and aggregation schemes. Specifically, many studies focus on a systematic review of methods [4], simulation tools [5], and challenges [6].

For UEMs, the modelling approach can be (1) top-down, using historical aggregated data for projection analysis, or (2) bottom-up, using disaggregated data for tracking technologies changes. In addition, bottom-up models subdivide into reduced and whole domain models. Reduced domain physical models are the most widespread method but have an inherent loss of variability [7]. The reduced domain approach groups similar buildings into classes and identifies a representative building for each. UEMs use data from this reference building to extrapolate results to its building stock. Reference buildings can be theoretical archetypes built on average data or real-reference buildings (RB) with characteristics similar to the median data. Whole domain models, also known as building-by-building models, use coarse representations of each building and its occupants [8]. Therefore, these are computationally intensive [9] and less suitable for energy-saving predictions.

Extensive datasets for reference buildings already exist. The most known are the cross-typology USA Department of Energy database [10] and the European residential typology matrix developed by the TABULA project [11]. Both datasets employed deterministic segmentation and simple classifiers such as building use, age and climate. Current research focuses on stock segmentation using machine learning algorithms and its comparison to standard practice. A study on the residential stock in Vienna assessed three segmentation methods under different

combinations of 17 classifiers. That study showed the adequacy of the K-means algorithm over hierarchical agglomerative clustering for annual heating demand prediction [12]. Similarly, another study compared K-means and K-medoids to segment a residential district in China [13]. For this district, k-medoids performed better even though its prediction differed only 1% from k-means for urban energy demand.

For UEMS, deterministic characterization is frequent in which the descriptive parameters take the mean values for the building stock. However, some studies use principal component analysis [14] and linear regressions [15] to improve features definition. Most noteworthy is the hierarchical calibration proposed for the propagation of uncertainty from building to urban scale for the Danish residential stock using Bayesian techniques [16]. That study assumed that archetype features are random variables within an underlying distribution function and thus enable the inference of uncertain parameters through sensitivity analysis. Seldom studies have dealt with UEMs for free-floating stocks whose buildings do not consume energy for air conditioning, contrary to conditioned building stocks. A project on social housing in Brazil identified two RBs from a sample of 120 houses using qualitative and quantitative data and validated its results against simulated degree hours [17]. Likewise, studies on the low-cost residential building stock in South Africa [18] and the residential stock in Chile [19] created deterministic archetypes from a tree-based segmentation of buildings' age, appearance, geometry, and occupancy profiles. However, these studies failed to validate their archetypes because of the lack of a quantifiable significant energy metric.

Following is a description of research gaps after a detailed review of reduced domain UEMs. Appendix A sums up that review. UEMs require an extensive dataset, but this information is usually non-existent, not up-to-date, or not available. Therefore, many studies rely on educated guesses [16,19] rather than factual data. Stock data consistently neglect building renovation, leading to discrepancies between buildings and their class [20]. Deterministic bins are the most

widespread segmentation technique because of their simpler classifiers and data availability. However, this technique results in an excessive number of archetypes and considerable intra-class heterogeneity [21]. Cluster techniques are better for multivariate classification though their adequacy for free-floating stocks is not proven [18]. In addition, national statistics serve for UEMs validation, but this does not apply to specific urban scales due to a lack of disaggregated data [22]. Aggregated quantification flattens building-level errors as studies report errors ranging from 1% to 19% for stocks and 55% to 99% for buildings [23]. Thus, there is an increasing concern that theoretical archetypes might not represent the performance of buildings [24].

To date, there is a better understanding of the residential stock than the non-residential [25,26], with the latter documented based on isolated buildings. The educational stock represents 17% of the non-residential sector in Europe and 18% of its energy consumption [27]. This stock differs in construction practices and age but has a reasonably homogeneous operation pattern. Despite its current high energy consumption, energy use intensity (EUI) in educational buildings will increase to provide adequate indoor comfort levels [28]. For this reason, there is the need to reduce its energy demand by deep-energy retrofitting. In this sense, many studies have assessed energy conservation measures (ECMs) for educational buildings [29,30] but failed to quantify their replicability. A study classified over 1110 Greek schools into five categories using k-mean clustering to predict their space heating demand [14]. Likewise, another project on 1857 Serbian schools selected 13 representatives RBs and predicted primary energy savings from 32% to 70% for its entire stock [31]. That study found broad discrepancies between collected data and the actual state of those buildings because of poor retrofit records. Clustering techniques assessed the cost-benefit ratio for energy interventions in the school stock in Lazio, Italy, predicting an average heating demand of 23 kWh/m² and energy savings of 30%, but showing considerable differences between simulations and measurements [32]. In a preliminary study, the authors

derived two building typologies from a sample of 130 schools in Quito, Ecuador using k-mean clustering but did not validate results for energy assessment [33].

This article aims to contribute towards a better understanding of the performance of educational stocks and their energy intensity and the establishment of energy baselines. For this reason, this research defines a reduced domain bottom-up physical model based on RBs which (a) proves suitable for free-floating and conditioned stocks alike, (b) relies on calibrated dynamic simulation models for energy assessment, (c) uses sensitivity analysis for assessing RBs' variability to urban boundary conditions, and (d) performs probability up-scaling for the aggregated energy demand. The first application of this model was to define energy building typologies for the educational stocks in Barcelona, Spain (conditioned stock) and Quito, Ecuador (free-floating stock). This study does not focus on these RBs energy performance but on their ability to represent their stocks. This study is part of a comprehensive research project to characterize the building surface-level performance and passive retrofitting alternatives using multi-objective optimization for energy savings, cost efficiency and comfort. The remaining sections are a) detailed description of the method, b) application on the two previously mentioned building stocks, c) discussion on the results, and d) final remarks.

2. Multistage methodology approach:

This stepwise methodology aims to extrapolate RBs energy performance to an urban scale through diversification and probability up-scaling processes to include urban boundary conditions. The typical steps for building archetypes selection are segmentation, characterization, quantification and validation [23]. However, this research performs validation before quantification to improve transferability among stocks. For this purpose, the validation step is done at the building level using statistical indexes and disaggregated data. Also, quantification includes energy demand sensibility to urban boundary conditions. This novel

methodology has three phases: 1) selection of RBs, 2) RBs energy modelling, and 3) stocks' energy demand quantification. Figure 1 shows a base scheme for this approach.

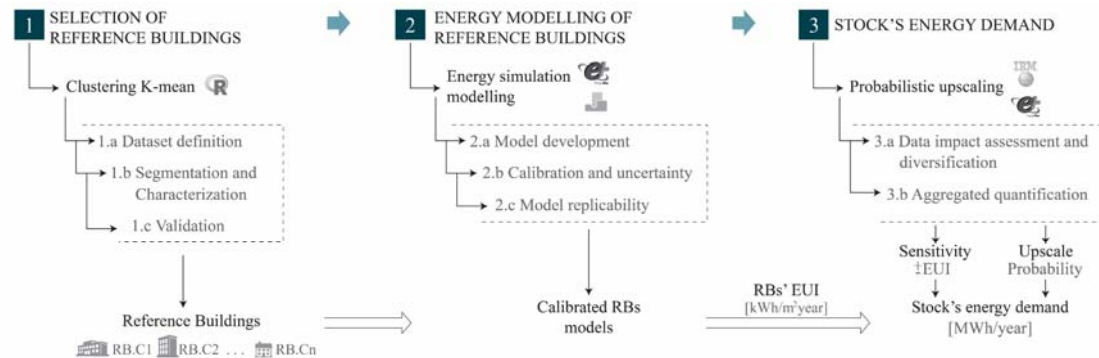


Figure 1 Stages and steps in the reduced-domain urban energy model

2.1 First stage: Selection of Reference Buildings

RBs are preferred because they permit detailed analysis and energy audits without losing the prediction, estimation and aggregation capability of archetypes [24]. For their selection, an obligatory first step is the collection of data, unless already available.

2.1.1 Building stocks datasets:

Building data compilation includes general and specific data. General data refers to the name, location, teaching schedule, education program, amongst others. Specific data refers to four customary aspects: form, envelope, systems and operation [10]. Regarding systems category, this refers specifically to each stock focusing on mechanical systems for conditioned building stocks and sanitary systems for free-floating. This data collection is step-by-step. First, official education datasets provide the number of institutions, students and building area. Second, building characteristics are retrieved from cadastre, geographic information systems (GIS), technical reports, or blueprints. Third, management authorities provide a list of completed retrofit interventions. Fourth, field visits serve to verify data and make amendments if necessary.

2.1.2 Stock segmentation and characterization:

Stock segmentation uses multivariate *K-means* clustering because of its adequacy for aggregated energy predictions [12]. *K-means* is a data-mining algorithm that identifies relations between objects – defined as vectors of $1 \times n$ features – and automatically assigns them into clusters by minimizing the distance between objects and their cluster centroid [34]. It requires the input of the “K” number of clusters defined in this study by maximizing their Calinski-Harabasz index. This index quantifies the intra-cluster homogeneity and inter-cluster heterogeneity and permits an unbiased selection of “K” contrary to size-based or modeller’s preferences approaches [14,32]. *R-language* runs the *K-means* algorithm with the following assumptions: Euclidean distance as similarity metric, random initialization centres, iterative process, and *K* defined by the maximum Calinski-Harabasz index for $k = 2$ to $k = 5$.

Clustering algorithms are exploratory techniques in which results depend on the features and metrics chosen. Therefore, the selection of the “*n*” features must pair well with the ultimate aim of the model. For *K-means*, the “*n*” features must be numerical, have a meaningful metric and allow normalization to avoid skewness in results. For educational stocks, sets of six features provide the best compromise between accuracy and modelling effort for energy predictions [35]. The six features chosen are: 1) ground floor area (m^2); 2) wall area (m^2); 3) thermal conductivity by walls (W/m^2K); 4) thermal conductivity by roofs (W/m^2K); 5) height (m); and 6) compactness ($1/m$), defined as the surface-to-volume index. Table 1 presents the calculation and recommended sources for these features.

Feature	Unit	Calculation	Source
Ground floor area (A_{gf})	m^2	Total area including external walls	GIS, blueprints
External wall area (A_w)	m^2	Area of walls in contact with external air	Blueprints, field surveys
U-value walls ¹ (U_w)	W/m^2K	Thermal resistance including lineal thermal bridges.	Construction details, technical codes
U-value roofs ¹ (U_r)	W/m^2K		
Height (H)	m	Flat roofs: top of ground slab to top of roof Pitch roofs: top of ground slab to ceiling	Blueprints, field surveys
Compactness (SV)	$1/m$	Surface area divided by enclosed volume	Blueprints

¹ Based in [36,37]

Table 1 Selected classifiers for the educational stocks

A review of classifiers used in over 25 UEMs is the basis to select these six features (see Figure 2) but considering only the most discriminating classifiers for educational stocks. Two variables usually describe form, one for building size and the other for building shape. U-value describes envelope's thermal properties because using age as representative of envelope's characteristics is meaningless for buildings preceding 1970 [12]. Operation features are disregarded as classifiers because schools have homogeneous occupation patterns and relatively low user control of their indoor environment; however, these features are included later for uncertainty analysis. Also, and as systems features have no impact on the thermal performance of free-floating buildings, these are excluded.

The selection of the optimal “n” features is beyond this study's scope, which selected six traits based on previous related research studies [35]. Although data analysis techniques, such as multilinear regression, may provide a more rigorous selection of optimum features to segment individual building stocks, this set of features would not be transferable amongst stocks. Therefore, individual segmentations sets are not appropriate for this bottom-up model objectives. Thus, these six classifiers are considered sufficient at this stage to perform stocks' segmentation. This segmentation is then evaluated regarding its goodness-of-fit and adequacy to represent buildings energy behaviour against dependent energy metrics.

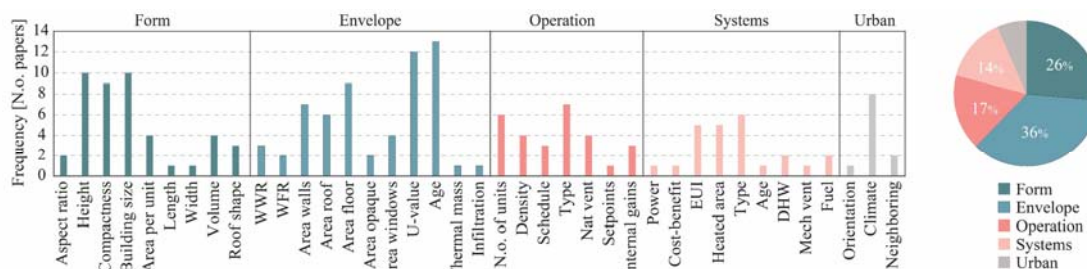


Figure 2 Frequency of classifiers in UEMs. Window-to-wall ratio (WWR), Window-to-floor ratio (WFR), Energy use intensity (EUI), Domestic hot water (DHW), Number of (N.o.)

Cluster's characterization is deterministic based on its centroid – vectors of $1 \times n$, where each variable is the mean of its cluster. This characterization is appropriate to determine RBs, though it is less precise than a probabilistic one [38]. RBs are the buildings whose Euclidean distance to their cluster centroid is the lowest (see equation 1). Clusters that represent over 10% of their stocks are considered significant.

$$D_{Si,Ck} = \sqrt{\sum \|Ck - Si\|^2} \in \mathbb{R}, \quad \text{where:} \quad \text{Eq.1}$$

$$Ck = [Af_k \ Aw_k \ Uw_k \ Ur_k \ H_k \ SV_k] \in \mathbb{R}^{1 \times 6}$$

$$Si = [Af_i \ Aw_i \ Uw_i \ Ur_i \ H_i \ SV_i] \in \mathbb{R}^{1 \times 6}$$

Where $D_{Si,Ck}$ is the Euclidean distance from each school to its centroid, C_k are their centroids and S_i their school building.

2.1.3 Clustering validation:

The proposed validation is two-fold: cluster validity and data-driven validity. Cluster validity uses several statistical indexes to evaluate the goodness of the clustering scheme used – number of clusters, algorithm and distance metric – compared to other clustering structures with different parameters. As clustering techniques are exploratory, the adequacy of their segmentation relates to the aim of the model. Previous studies have used cluster validity indexes to validate building benchmarking and typology classification [14,39]. Total Error Sum of Squares (TESS) and Silhouette indexes represent the intra and inter-cluster variability, respectively; their validation criteria was the maximum inflexion point for the TESS index and the maximum value for the Silhouette index. These indexes are calculated for $k = 1$ to $k = 5$ and three distance metrics: Euclidean, Manhattan and Mahalanobis. To further increase the confidence in clustering results, the NbClust package in *R-Language* [40] computes over 30 cluster validity indexes and assesses the best segmentation scheme.

The proposed data-driven validity involves comparing a dependent energy metric between RB and the building-by-building data for its cluster. RBs are valid if their performance is close to the

median of their cluster. A previous study proposed a similar approach but with less stringent conditions to validate free-floating archetypes [17]. The energy metrics used are a) EUI for conditioned stocks and b) the number of hours in thermal comfort for free-floating stocks. Thermal comfort is defined as in adaptive comfort standards [41,42]. Empirical data is preferable to calculate these metrics, but because of privacy issues and timeframes, this is not always possible to attain. In these cases, simple simulation models provide the required data. Single-zone dynamic simulation models for each school are created in *Design Builder* and configured to display real geometry, envelope, urban setting, and occupancy parameters. These simple models do not provide sufficient data for their performance evaluation but suffice for the goodness-of-fit evaluation.

2.2 Second stage: Energy Modelling of Reference Buildings

Detailed dynamic simulation models are constructed for each validated RB and are subject to calibration before up-scaling. Building energy modelling is chosen because it allows analysts to fully quantify the energy consumption for a building without historical data and to simulate sub-hourly behavioural patterns needed for naturally ventilated buildings [43].

2.2.1 Energy model development

RBs multiple thermal zone models are constructed in *Design Builder*, including personalized profiles for each zone, shadows from the surrounding environment, custom-made weather files, and calculated infiltration and ventilation rates. Building and occupancy parameters collected in-site are detailed in [Appendix B](#). Blueprints constructed from site surveys set the basis for the building models and include geometry, space distribution, fenestration area, operable area, and location of active mechanical equipment. The envelope thermal transmissivity is measured with heat-flux meters during peak winter week to maximize temperature gradient. Non-lineal thermal bridges are modelled in *Therm*, a two-dimensional heat-transfer modelling tool [44], and set in *Design Builder*. The distribution of luminaries and lamps nominal power is collected

on-site to calculate the lighting power density. The maintenance crews provide mechanic equipment specifications, antiquity and operation schedules. Sub-hourly schedules are constructed from surveys to teaching and maintenance staff for windows, lighting, shadow devices operation. Occupancy density corresponds to the number of students in each classroom and the number of desks in each office.

Classrooms are monitored for three months to evaluate their indoor environmental conditions – air temperature and relative humidity – with the specific monitoring periods as allowed by the school’s administration. Dataloggers are placed in representative classrooms throughout the monitored schools at ceiling level to avoid tampering. The monitored classrooms are selected based on their location and specific issues reported by the school’s administration, with the number of classrooms monitored depending on school size and availability. Weather data is retrieved from the nearest available meteorological station and converted to *epw* simulation weather files. Most stations do not provide direct and diffuse components for solar radiation nor dew-point temperatures. The Perez DIRINT model in MATLAB breaks down the global horizontal radiation into direct and diffuse [45]. Magnus formula calculates the dew-point temperature.

Some parameters cannot be measured on-site or would require testing procedures beyond this project’s scope. These parameters include infiltration and ventilation rates, equipment normalized heat gains, domestic hot water (DHW) rates, and materials’ thermal properties. The airflow rates were calculated using the “calculated natural ventilation model” in *Design Builder*. This model requires: 1) windows operable area, 2) operation profiles, and 3) surface crack data. The authors defined the first two parameters during building inspection as described above, while the crack data – infiltration – definition is based on technical literature [46,47]. Equipment normalized gains are set according to local energy codes [48] or international standards [49]. For schools with DHW, the consumption rate is set to 4 l/day/person [48]. The specific properties

of the materials are set according to local construction codes [47,50] or ISO standards [51] and calibrated to match the measured thermal transmissivity. The range for the metabolic rate for children in classroom activities is taken from [52]. Ventilation, heating and cooling setpoints are extrapolated from interpolation between operation schedules and indoor environmental monitoring data. This interpolation results in plausible ranges but no set values.

2.2.2 Uncertainty and model calibration

Sensitivity and uncertainty analyses evaluate the impact that the non-measured model parameters have on its predictability. The sensitivity analysis informs the stepwise calibration, and the uncertainty analysis serves to set suitable values for model calibration. Six relevant parameters are evaluated: occupancy density, infiltration rate, metabolic rate, natural ventilation setpoint, heating setpoint, and operation of shading devices. Ideally, calibration should be for all uncontrolled parameters, but this would be unfeasible because of data limitations [16]. These six parameters are selected based on their recognition as significant sources of uncertainty [53]. The values for these parameters are unknown, but their variability range is determined from literature or experimentally, as explained above. The numerical range and steps to evaluate each variable are in Table 2.

Parameter	Description	Unit	Step	Range
Density	Number of students per classroom area	people/m ²	0.05	0.4-0.95
Infiltration¹	Uncontrolled airflow per length of window	m ³ /h/m	0.5	0-5
Metabolic rate²	Heat rate in typical classrooms activities	W/person	5.0	63-90
Natural ventilation setpoint	Temperature-driven windows' opening	°C	0.5	19-24
Heating setpoint³	Base air temperature for winter heating	°C	0.5	19-22
Curtain operation	Radiation-driven internal shadows operation	W/m ²	100	100-700

¹ Using crack templates, base values [46,47]

² Values from [52]

³ Ranges from [46,54]

Table 2 Uncertainty sources in model calibration, ranges and steps

Standardized and unstandardized beta coefficients identify the influence of each variable in the simulation process and quantify its impact. Multi-linear regressions compute these coefficients between the six studied parameters and their root mean squared error (RMSE) in indoor temperature prediction. Each variable is calibrated individually, and its ultimate value for the energy models is the one that has the highest reduction in the RMSE. This calibration is done manually, starting with the variable with the highest standardized beta coefficient. The final simulation models calibration follows the error metrics in ASHRAE 14 Guideline for energy calibration [55] - normalized Mean Bias Error (nMBE) and Coefficient of Variance of Root Mean Square Error (CvRMSE) - but with more stringent thresholds as suggested in literature $\pm 2\%$ for nMBE and $\pm 10\%$ for CvRMSE [56].

2.2.3 Model replicability

After model calibration, the following standardizations are made: average density of students in classrooms based on local standards, official working schedules, heating and cooling setpoints according to Category 2 in EN 16798-1 [41], natural ventilation setpoint set 2 °C above the heating setpoint, operation under full conditioned mode during occupancy hours, and use of Test Reference Year weather files [57]. In free-floating stocks, and to estimate their energy demand, active systems are set to standard local practices and their coefficients of performance (COP) as mandated by enforced energy codes. This standardization facilitates the comparison between RBs and aid in their direct up-scaling [15].

2.3 Third stage: Quantification of the stocks' energy demand

The diversification approach and probability up-scaling give back the loss variability in the reduced domain approach regarding the RBs' urban boundary conditions. For calibration, RBs models include their urban environment. These boundary conditions are not predominant for the building stock. As such, RBs performance is evaluated under different urban scenarios as follows.

2.3.1 Impact assessment for urban boundary conditions and RBs' diversification

Multi-lineal regressions techniques assess the variability in the RBs' EUI due to three urban parameters: orientation, site elevation, and built-up density. These parameters are tested in discrete steps of 45° for orientation, 50 m for elevation, and 2500 m²/ha for built-up density. Minimum and maximum values are topography limits for elevation and 0 to 20000 m²/ha for built-up density. The latter is calculated as the total building area per unit of land area (1 ha) and describes the variability in the surrounding buildings' distribution and height. Plot size and shape are the ones from the RBs, but the urban boundaries are the most frequent in each stock regarding urban layout, street canyon, and open or green space. These three parameters provide the first assessment regarding urban variability and its inclusion in probability up-scaling, although these parameters cannot reflect the full spectrum of urban conditions.

Up-scaling requires the creation of "categories" by combining the previously mentioned three urban parameters. Beta coefficients rank these variables to include only those discriminating in the categories. These categories generate a new set of energy simulations with diversified EUIs. Joint probability distributions predict the probability of these categories occurring in the assessed stocks. Their calculation is as follows. First, GIS specify these three variables values for each school in the datasets [58–60]. Second, the independent probability for each variable is calculated. For example, the number of schools in low (<7500 m²/ha) urban built-up density divided by the total number of schools. Last, the joint probability is the product of these independent probabilities.

2.3.2 Aggregated quantification

Up-scaling uses the metric EUI (kWh/m²year) as it is better suited to compare typologies. For stock energy quantification, the standard approach - dubbed as non-diversified - is the product of RBs' EUI and their clusters' area (see equation 2). The diversified approach considers the probability distributions for urban boundary conditions, the diversified RBs' EUI and the clusters'

area (see equation 3). This diversification keeps the RBs reductive modelling and improves stocks aggregated quantification. The latter by including previously unconsidered parameters.

$$Q_{ND} = \sum_{k=0}^k (EUI_k A_k) \in \mathbb{R} \quad Eq.2$$

$$Q_D = \sum_{k=0}^k \left[\left(\sum_{i=0}^i EUI_{k,i} f_i \right) A_k \right] \in \mathbb{R} \quad Eq.3$$

Where Q_{ND} is the stock's non-diversified energy use, Q_D is the diversified energy use, k is the number of clusters, EUI_k is the EUI of the RB for each cluster, A_k is the total building area for each cluster, i is the number for probability outcomes, $EUI_{k,i}$ is the EUI of the RB in each probability scenario, and f_i is the frequency distribution for each probability outcome.

2.4 Case Studies

This multistage approach was applied first for the public educational stocks in Barcelona, Spain and Quito, Ecuador. These stocks have considerable differences in age, size, occupancy density and operation mode (see Table 3). This study builds upon previous work describing these stocks [61]. The number of public schools varies significantly, with 159 and 268 in Barcelona and Quito, respectively [62,63]. Appendix C details this study data collection, sources, and references. Data collection was from the beginning of 2018 until January 2020. Both cities' governments have recognized the need for deep retrofitting their educational centres but with different end goals, energy reduction in Barcelona [46] and health issues in Quito [64]. Considering retrofit as end-goal, new and fully renewed buildings were not included for stock classification as neither were historically listed buildings because of their specificity.

		Barcelona (BCN)	Quito (UIO)
General			
Climate ¹		Mediterranean	Highlands
Teaching schedule	[weeks]	34 + 2 compact	40 + 4 half
Holidays	[days]	118	85
Size per school	[m ²]	3318	2297
Number of students per school		263	1035
Stock			
Number of schools		159	268
Incomplete information		1	8
Sharing infrastructure ²		4	7
Listed buildings		22	19
New built ³		37	20
Marked for demolition		3	0
Total schools for classification		92	214
Total construction area	[m ²]	301012	741629

¹ According to Koppen classification
² Between schools or with other public services
³ 2006 set as baseline because of the new energy code in Spain and the renewal campaign in Ecuador

Table 3 General description for the two educational stocks

A substantial proportion of Barcelona's stock precedes the first Spanish energy building code of 1979. Most schools are compact, low-rise concrete-frame buildings poorly insulated with high glazing ratios. An ongoing project for near-zero energy schools characterized 282 centres in the Barcelona Metropolitan Area into four shape models [65]. The three showcase buildings had energy consumptions between 90 to 150 kWh/m²/year, way above the median of 64.32 kWh/m²/year. This deviation shows the need for a multivariate classification approach. The school stock in Quito is more homogeneous regarding shape and materiality but varies significantly in building size. It is relatively newer, with most buildings dating from the 1980s. In 1995, a seismic-resistance study characterized Quito's stock into two typologies: concrete-frame two-story buildings and lightweight metal-frame classroom units [66]. On the current quality of classrooms, problems relate to daylight, ventilation and thermal comfort. Over 30% of students complaining of suboptimal thermal comfort [67], but the energy demand for air conditioning in this stock has not been quantified.

3. Results

This section follows the aforementioned multistage approach for each case study and presents their 1) stock classification and RBs selection, 2) RBs energy modelling, and 3) urban energy quantification.

3.1 First stage: selection and validation for reference buildings

Figure 3 shows segmentation results and selected RBs. Calinski-Harabasz index favoured four and two clusters for Barcelona and Quito's stocks, respectively. This cluster scheme had the best results in TESS and Silhouette indexes (see Appendix D). Although there were no outliers in the studied samples, verified by a cumulative probability in a chi-square distribution of Mahalanobis distance, cluster four in Barcelona was not representative because it groups very singular shaped buildings and less than 10% of the stock's area. There is a more significant inter-cluster heterogeneity for the sample in Quito than for the three significant clusters in Barcelona that have similar inter-distances between them. Clustering disaggregates relatively similar shaped and age buildings into different categories because of retrofit interventions in their thermal envelopes. Therefore, it signals the importance to consider building stocks in their as-is state despite the substantial effort for data compilation.

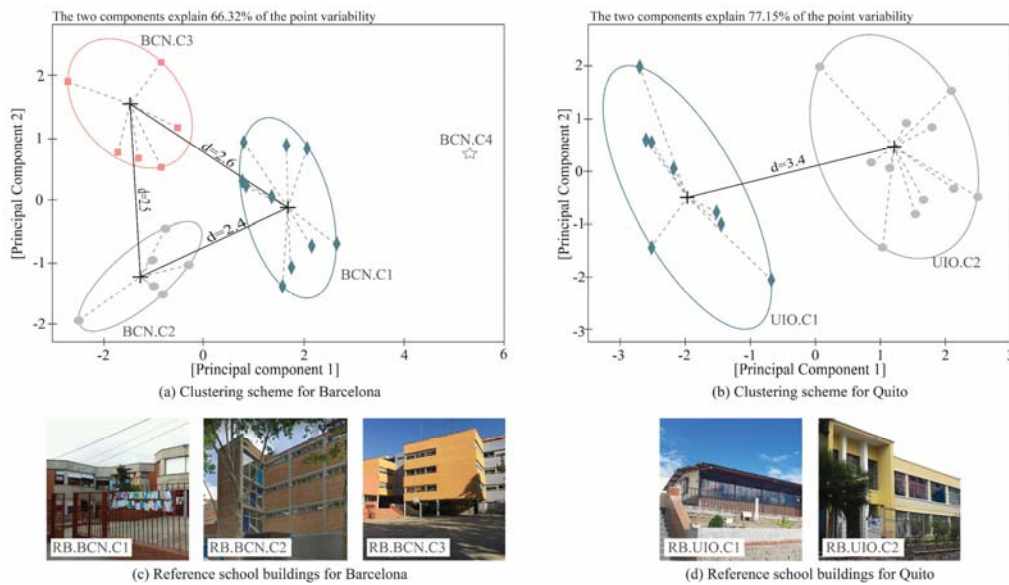


Figure 3 Clustering graphical representation using principal components analysis for a) Barcelona and b) Quito; selected RBs in c) Barcelona and d) Quito. For identification the following nomenclature has been used: for clusters (CITY_ID.C_NUMBER), for RBs (RB.CITY_ID.C_NUMBER)

For both cases, clusters differ significantly in floor area, height, compactness and U-value of roofs (see p-values in Table 4). Surface area and U-value of walls do not influence the outcome

for Quito, suggesting that fewer classifiers would produce similar results. In contrast, all variables are significant for Barcelona, which reflects its heterogeneity. Correlations between features were revised for a p-value < 0.05. P-value showed that for schools in Quito, shape and materiality are highly correlated. In Barcelona, there are no correlations between variables. Therefore, building typologies are less easily identifiable and less suitable for deterministic bin segmentations. In fact, by using $k = 2$ and $k = 3$ for Barcelona, the school's assignation varies significantly between clusters, whereas for Quito, clusters only subdivide.

Table 4 shows the cluster characterization using their centroids; standard deviations are included for data completeness. Clusters BCN.C1 and BCN.C2 share similar envelope characteristics but differ in their shape and distribution schemes. BCN.C1 comprises stepped low-rise compact buildings distributed around a central courtyard, and BCN.C2 groups mid-rise schools, with one or more rectangular edifices. Cluster BCN.C3 is less homogenous and includes buildings with various shapes but lower thermal conductivity walls and higher conductivity roofs than previous clusters. In Quito, school typologies differ more significantly. UIO.C1 are single-story modular lightweight structures and UIO.C2 multi-story concrete-frame buildings. A close review of this stock showed that most schools have buildings belonging to either typology and that clustering favoured the dominant one. Therefore, the individual analysis for each building in a school could provide better segmentation.

	Agf [m ²]	Aw [m ²]	Uw [W/m ² K]	Ur [W/m ² K]	H [m]	SV [1/m]	Units [N.o.]	Area [m ²]	Freq. [%]
BCN.C1	1410.6	2062.2	1.36	0.95	7.5	0.47	31	97236.1	32.3
	$\sigma \pm 171.7$	$\sigma \pm 550.8$	$\sigma \pm 0.2$	$\sigma \pm 0.3$	$\sigma \pm 1.04$	$\sigma \pm 0.07$			
BCN.C2	791.10	1985.1	1.38	0.96	10.97	0.43	26	88601.7	29.4
	$\sigma \pm 106.3$	$\sigma \pm 177.3$	$\sigma \pm 0.2$	$\sigma \pm 0.4$	$\sigma \pm 1.56$	$\sigma \pm 0.04$			
BCN.C3	1155.4	2667.2	1.02	1.56	10.1	0.42	24	86298.1	28.7
	$\sigma \pm 124.5$	$\sigma \pm 554.9$	$\sigma \pm 0.3$	$\sigma \pm 0.3$	$\sigma \pm 1.59$	$\sigma \pm 0.04$			
p-value	0.000	0.008	0.023	0.017	0.000	0.000			
UIO.C1	1314.0	1266.3	2.46	3.45	3.00	1.04	112	302480.3	40.5
	$\sigma \pm 270.7$	$\sigma \pm 179.0$	$\sigma \pm 0.16$	$\sigma \pm 0.11$	$\sigma \pm 0.30$	$\sigma \pm 0.10$			
UIO.C2	713.5	1190.4	2.49	3.00	5.66	0.63	102	439149.0	59.5
	$\sigma \pm 150.1$	$\sigma \pm 319.4$	$\sigma \pm 0.20$	$\sigma \pm 0.31$	$\sigma \pm 0.41$	$\sigma \pm 0.05$			
p-value	0.000	0.517	0.783	0.000	0.000	0.000			

Ground floor area (Agf), Wall area (Aw), U-value walls (Uw), U-value roofs (Ur), height (H), compactness (SV)

Table 4 Characterization and frequency distribution for the clusters

The selected RBs were validated against a dependent energy metric relevant to each stock, EUI for Barcelona and hours in thermal comfort for Quito (see section 2.1.3). Barcelona's local government provided annual data for 2018 on electricity and gas consumption for a representative sample of its schools. These values were normalized regarding building area previous to their use in this study validation. For Quito, single-zone simulation models of each school in a sample were developed to calculate indoor temperature and evaluate thermal comfort conditions. Most designated RBs showed values very close to the medians of their respective clusters, fulfilling the required validation. The exception was the RB for cluster BCN.C3, which performed significantly better than its cluster (see Figure 4). Table 5 describes the four validated RBs. Barcelona's RBs represent 61.7% of its stock, whereas Quito's RBs represent its entire stock.

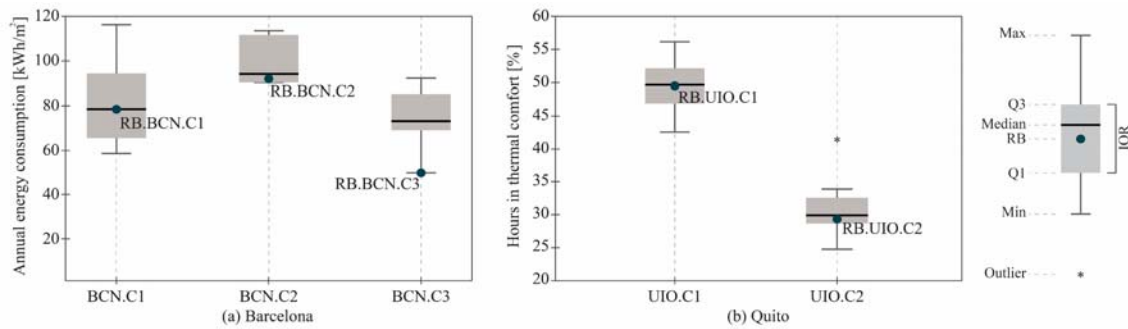


Figure 4 Data-driven validation for real-reference buildings (RB). The RBs are marked to see how each RB behaves with respect to its cluster. Maximum data point excluding outliers (Max), minimum data point excluding outliers (Min), first quartile (Q1), third quartile (Q3), interquartile range (IQR).

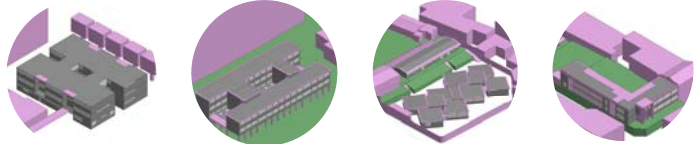
PARAMETER	UNIT	RB.BCN.C1	RB.BCN.C2	RB.UIO.C1	RB.UIO.C2
Age		1976	1972	1976	1990
Gross floor area	[m ²]	3563	2683	1476	1580
WWR	[%]	30.0	25.2	29.5	21.3
S/V	[1/m]	0.53	0.66	0.92	0.54
Occupancy density	[people/m ²]	0.4-0.5	0.4-0.5	0.65-0.95	0.55-0.85
Use hours		9am-16:30pm	9am-16:30pm	7am-12:30pm	7am-18:30pm
Walls	[W/m ² K]	1.43	1.32	2.27	1.81
Roof	[W/m ² K]	0.23	0.39	6.45	2.31
Ground floor	[W/m ² K]	1.79	2.56	2.38	3.04
Internal floor	[W/m ² K]	1.18	1.70	-	2.15
Glazing	[W/m ² K]	5.77	5.77	5.89	5.89
Infiltration rate	[m ³ /h m]	1.0	0.5	4.0	2.0
Shading devices		Roller shutters	Roller shutters	None	Curtains

Table 5 Geometrical and thermophysical characteristics for the validated RBs. Window-to-wall ratio (WWR), surface-to-volume index (S/V)

Even though the lower EUI for the RB in cluster BCN.C3 could be due to better operational practices – some studies have shown the considerable impact of operation practices in EUI [68,69] – current data does not justify this hypothesis. In addition, the distance of this RB to its cluster centroid is 1.5 times larger than for any other RBs. Accordingly, this RB is not representative of the composite characteristics of its cluster and, therefore, was not further considered. A further subdivision could improve this cluster representation. For this, segmentation requires classifiers more appropriate to the reduced sample [35].

3.2 Second stage: energy behaviour in the reference schools

Information collection for the detailed simulation models was on-site during 2019. Table 6 summarizes the energy models' input parameters, and Appendix E fully describes them. Quito's schools were monitored from April to June and Barcelona's from September to December as allowed by their local governments. Calibration was successful for all RBs. However, building RB.UIO.C1 had the highest RMSE with a value of 1.24 °C. Significant errors occur at noon because of peak heat flux and the end of school hours. Both causes produce high thermal dynamics that the simulation models cannot reflect. Despite this, this school model has the second-lowest nMBE proving this index is prone to cancellation effects. For Barcelona, validation was further reviewed to monthly gas bills for 2019 to test the accuracy of our approach. This revision resulted in estimation errors of 4.70% for RB.BCN.C1 and 4.52% for RB.BCN.C2, compliant with ASHRAE thresholds.



System	Parameter	Units	RB.BCN.C1	RB.BCN.C2	RB.UIO.C1	RB.UIO.C2
Heating	Type		GB + water radiators	GB + water radiators	(GB + water radiators)	(GB + water radiators)
	COP		0.7	0.865	(0.92) ¹	(0.92) ¹
	Setpoint	[°C]	22	21	(20) ²	(20) ²
	Operation		Nov-Mar	Nov-Mar		
	schedule		8:00-17:00	7:30-21:00		

Cooling	Type		Splits	(Multi-splits)	(Multi-splits)	(Multi-splits)
	COP		2.5	(2.6) ¹	(2.6) ¹	(2.6) ¹
	Setpoint	[°C]	25	(25) ²	(24) ²	(24) ²
	Operation schedule		Jun-Sep 10:00-17:00			
DHW	Type		Electric heater	Gas Boiler ³	None	None
	Rate	[l/day·ppl]	4 ¹	4 ¹		
	COP		0.85	0.81		
Ventilation	Setpoint	[°C]	24	23	21	22
	Operation schedule		11:00-16:30	11:00-16:30	9:00-12:30	9:00-12:30
Lighting	Type		FL	FL	LED/FLC	LED
	Power density	[W/m ²]	8.6	8.6	2.25/7.05	2.25
	Power density					
Equipment	Power density	[W/m ²]	4.5 ¹	4.5 ¹	None	None
Calibration	Iterations	[#]	44	39	34	40
	nMBE	[%]	-0.67	0.26	0.52	0.81
	CvRMSE	[%]	4.76	4.96	6.42	5.06
	RMSE	[°C]	1.12	1.11	1.24	1.02

¹ Reference values from [48]

² Reference values from [41]

³ Dedicated natural gas boiler

Table 6 Parameter inputs and calibration indexes for these simulation models. Values in () represent hypothetical systems used for thermal demand calculations. Fluorescent lamps (FL), compact fluorescent lamps (FLC).

Figure 5 depicts the sensitivity analysis and the influence that the six uncontrolled parameters had on the models' outcome. Heating and natural ventilation setpoints impact the most, followed by occupancy density. The heating setpoint uncertainty was highly relevant as the only control thermostat in the studied schools was the boilers, with setpoints reported between 55 °C to 60 °C. A one-degree increment in heating setpoint produces indoor temperature increments of 0.11 °C for RB.BCN.C1 and 0.17 °C for RB.BCN.C2. Natural ventilation uncertainty owes to the differences in windows operation, as reported in field surveys. Cross-referencing surveys to indoor temperature showed that windows operation is mapped better through a control setpoint contrary to unified schedules used in the literature [70]. This setpoint was 22 °C for Barcelona and 21 °C for Quito, with an amplitude of ± 2 °C. Variations of one degree in this setpoint generate temperature fluctuations of 0.13 °C to 0.18 °C. Discrepancies in occupancy density among classrooms produced changes in sensible heat gains of 12.58 W/m² in Barcelona and 37 W/m² in Quito. The latter is due to differences of up to 12 students per classroom and their smaller classroom size. Increasing one student per surface area leads to an increment in indoor temperature of 0.56 °C, 0.36 °C, 0.91 °C, and 0.46 °C for the four studied RBs.

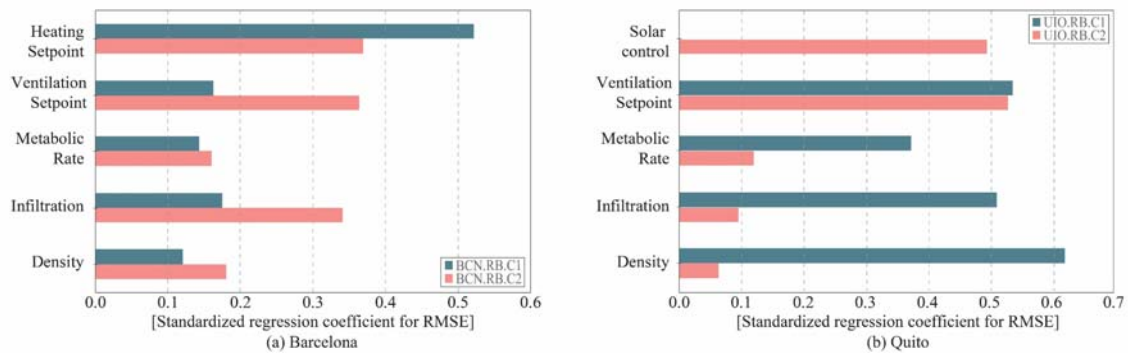


Figure 5 Sensitivity analysis for sources of uncertainty in the modelling for the studied RBs. Root mean square error between measured and simulated temperature (RMSE)

Uncertainty analysis narrowed down the ranges for the uncontrolled parameters and set the most appropriate values for model calibration (see Tables 5 and 6). The average prediction uncertainty for all models was below ± 0.6 °C; however, it reached maximums of ± 3.30 °C during specific hours in the models for Barcelona. This considerable uncertainty occurs during the non-occupancy periods as surveying did not account for these. Therefore, auditing non-occupancy periods would improve the models' annual predictability. Despite the deterministic characterization, the prediction capability of these models had a 1:1 relation between measured and simulated data. Thus, these models neither over nor under-predict their outcome. In addition, the authors validated the simulation outcomes for a week outside the three calibration months. During this week, the simulation errors complied with the set thresholds. Figure 6 shows the measured and simulated data for RB.BCN.C1 alongside the prediction of indoor temperature for the last week of January 2020 (Appendix F depicts this data for the other RBs).

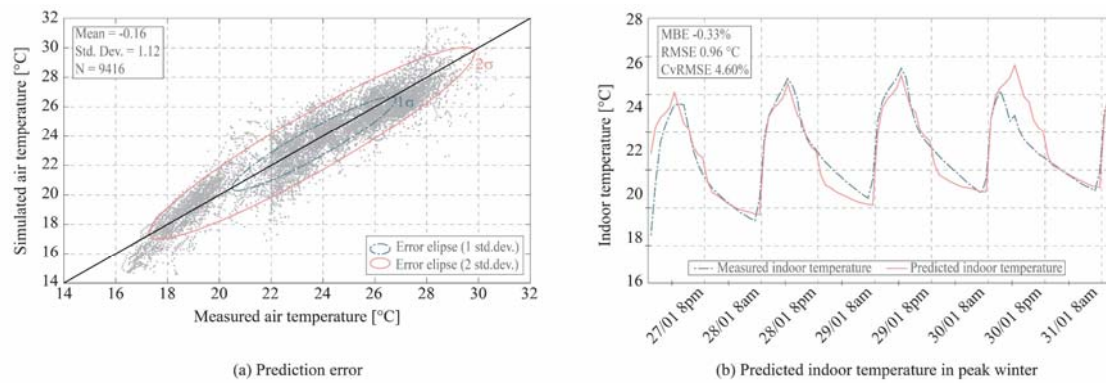


Figure 6 Simulation error for RB.BCN.C1 during (a) 3-month calibration period and (b) 1-week prediction period. Mean bias error (MBE), root mean square error (RMSE), coefficient of variance of the root mean square error (CvRMSE), standard deviation (Std. Dev.)

Stock segmentation emphasized the buildings' thermophysical characteristics. Therefore, these were assessed more explicitly. Figure 7 depicts the RBs' thermal balance and indoor temperature. For Barcelona, both RBs have a relatively similar thermal balance, but for RB.BCN.C1 horizontal envelop elements contribute less. Envelope losses surpass gains by 3 to 1 during winter and account for half the heat gains in summer, as typical for buildings in Mediterranean climates [54]. The recorded winter air temperatures ranged from 17 °C to 25 °C, hinting at overheating problems as detected in [71]. This high temperature is because of occupancy gains, continuous heating operation, and lack of zone controls.

For Quito, the most notable difference between RBs is due to their roofs. Roofs contribute heat gains for RB.UIO.C1 and heat losses for RB.UIO.C2. High heat gains in both RBs suggest the potential for heat storage and passive heating systems to diminish low temperatures at night. Despite an 18 °C average indoor temperature, during the first school hours, it drops to 13 °C, and at noon it rises to 30 °C. Winter-low and summer-high indoor peak temperatures in Barcelona are comparable to peak temperatures during a typical school day in Quito. The assessment of efficient ECMs requires considering this high thermal amplitude. Hence, additional research is needed to evaluate passive conditioning techniques. Few projects deal with the performance of free-floating buildings, despite their potential in the equatorial

highland climate. In contrast, many studies focus on the energy efficiency of schools in Mediterranean climates [72–74].

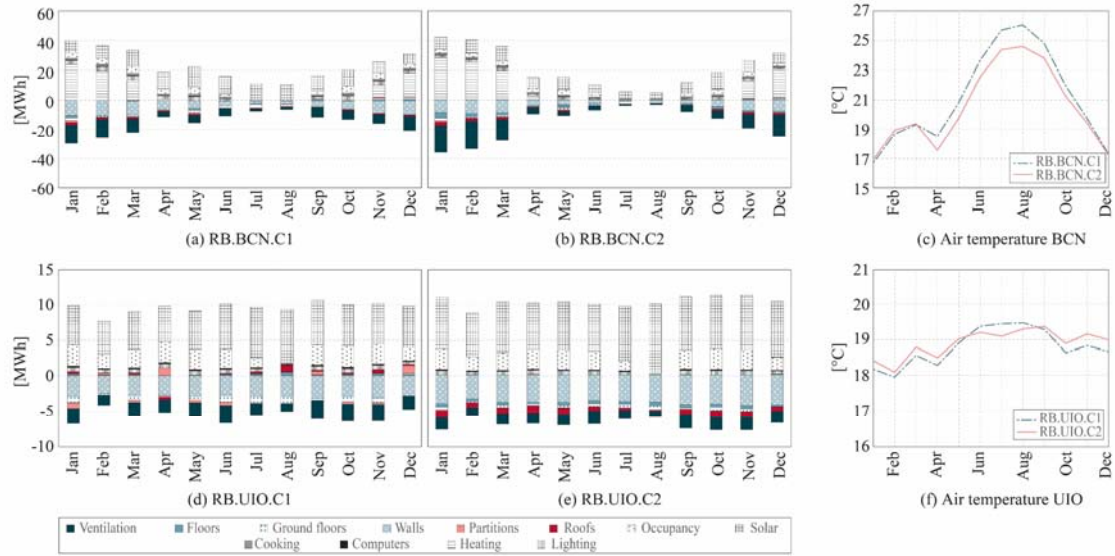


Figure 7 Monthly thermal balance (left) and indoor temperature (right) in studied RBs

Though the calibrated building models allowed for an extensive assessment of their current state and renovation strategies, their analysis was beyond this study's scope. For the stocks' energy demand quantification, the theoretical EUI for the RBs was calculated in full conditioning mode and with standard occupation parameters as described in section 2.2.3. When non-existent, the active systems were set as described in Table 6. Figure 8 displays the estimated EUI for the four RBs and their contributors. EUIs reflect the differences between case studies and building typologies. Since cooling load is low in Barcelona, both RBs have relatively similar EUIs to the statistical means of their clusters. End-use energy data revealed discrepancies between electricity consumption in Barcelona's clusters and RBs, with their models under-predicting it by 25% (5.25 and 5.4 kWh/m² in BCN.C1 and BCN.C2). However, natural gas consumption prediction has only a 2% error. Electricity disparity is because the simulation model did not include outdoor lighting. Nevertheless, outdoor lighting is not relevant to these buildings' thermal performance. Thus, it did not affect the diversification process, and simple extrapolation could include it in the up-scaling process.

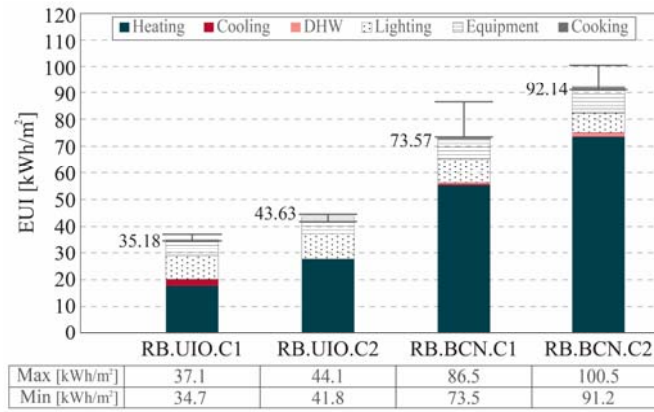


Figure 8 Energy use intensity (EUI) for the studied RBs and its variability due to urban conditions

3.3 Third stage: educational stock's energy use – diversified up-scaling

EUI increases from the calibrated RBs baseline because of variations in urban boundary conditions (see Figure 8). School RB.UIO.C2 is the only one that has lower and higher EUIs under different urban scenarios. The lower EUI occurs since RB.UIO.C2 is a row building in a medium-density neighbourhood, whereas the other RBs are detached buildings in low built-up density areas. Urban boundaries alter RBs' EUI by 20% with nominal maximum changes of 9.95 kWh/m² for RB.UIO.C2, 12.95 kWh/m² for RB.BCN.C1, and 22.37 kWh/m² for RB.BCN.C2. School RB.UIO.C1 has a maximum change of 6.8% because its modular distribution levers out the variations. In contrast, linear facades cause larger fluctuations in the other RBs. This fluctuation is because their performance depends on orientation and urban shadowing.

Regarding the studied urban parameters, elevation had no statistical significance ($p > 0.05$) as the simulation engine only considers it for pressure and natural ventilation calculations. Table 7 shows the regression coefficients and p-values for the three urban variables and each RB. Built-up density is significant for all cases, whereas orientation only for RB.BCN.C1 and RB.UIO.C1. Orientation lesser influence is due to the high glazing ratio in internal courtyards in RB.BC.C2 and the enclosed layout in RB.UIO.C2. In urban stocks where variations in environmental temperature and global horizontal radiation are significant, including diversified weather files should be explored. Such is the case of Quito, where weather monitoring showed hourly

differences between north and south zones of the city of 2.5 °C in temperature and 22.3 Wh/m² in solar radiation. Additional parameters to be considered are urban layout, building adjacency and street canyon. All of which were fixed in this project.

	RB.BCN.C1			RB.BCN.C2			RB.UIO.C1			RB.UIO.C2		
	β	<i>B</i>	<i>p</i>	β	<i>B</i>	<i>p</i>	β	<i>B</i>	<i>p</i>	β	<i>B</i>	<i>p</i>
Orientation	0.50	21.63	0.00	-0.22	-9.40	0.24	-0.22	-1.89	0.01	-0.07	-2.36	0.22
Elevation	-0.05	-3.77	0.70	0.00	0.07	0.99	-0.06	-0.38	0.51	-0.07	-2.05	0.22
Density	0.46	0.37	0.00	0.29	0.31	0.11	0.84	0.12	0.00	0.94	0.75	0.00

Standardized Beta coefficient (β), Unstandardized beta coefficient (*B*), and probability value (*p*)

Table 7 Regression coefficients for urban parameters on the RBs' final EUI

Since elevation was insignificant, orientation and built-up density combined to create twelve urban categories. Ranges for orientation were $\pm 45^\circ$ from the ordinal directions, and for built-up density were low (2500-7500 m²/ha), medium (7500-12500 m²/ha) and high (12500-17500 m²/ha). These twelve categories represent a compromise between diminishing the error in the EUI estimation and increasing the probability of each. The twelve categories had individual probabilities below 19%, whereas, with 24, the probability was below 12%, with 72, below 9%, and with 96, below 6%. The prediction error for the twelve categories was less than 4 kWh/m². For numerous building stocks, their categories joint probability distributions should be calculated for each cluster rather than for the building stock. However, because of the small populations in these clusters, it was not possible to do so. [Figure 9](#) depicts the individual probabilities and EUIs for each urban category and RB. The names for these categories are the ordinal direction followed by the built-up density, e.g. NE.L refers to northeast facing buildings in low built-up density areas.

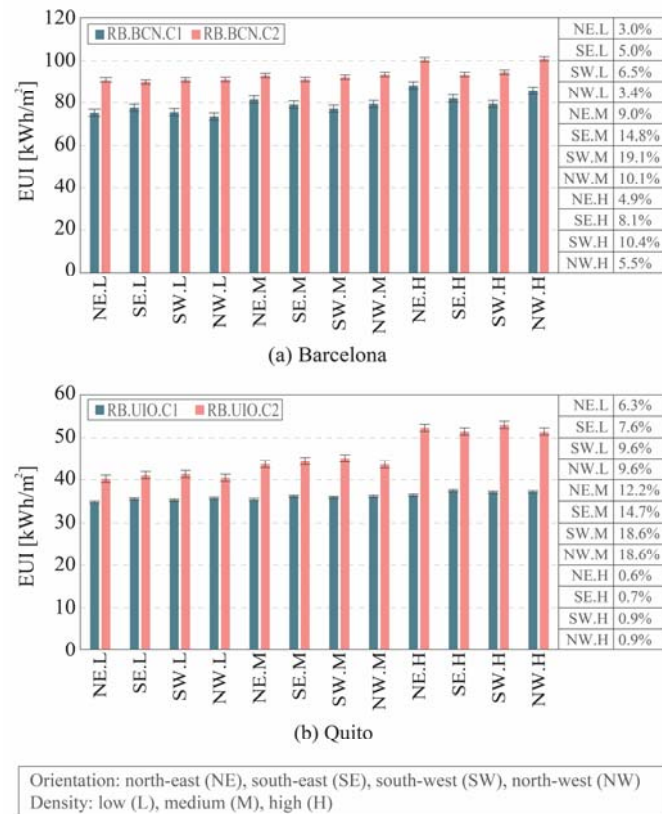


Figure 9 Urban-diversified energy use intensity for the studied RBs

Interestingly, the urban layout for RB.BCN.C1 was only similar to that of 13% of schools in this cluster. Moreover, the most predominant urban conditions increased this RBs EUI by 6.08 kWh/m²year. For all other school typologies, their RBs had similar urban layouts to most of their clusters which resulted in variations below 5% for the diversified EUIs for 90% schools in cluster BCN.C2, 70% in UIO.C1, and 64% in UIO.C2. The highest variability in EUIs estimation occurred for RB.BCN.C1 and RB.UIO.C2 with maximum deviations of 14.83 kWh/m² and 12.84 kWh/m². Urban shadowing has a large negative impact on these two schools because of their single-sided window layout and longitudinal facades. School RB.BCN.C2 has a variability below 12% (8.36 kWh/m²) and school RB.UIO.C1 below 8% (2.70 kWh/m²). School RB.BCN.C2 high WWR in its internal courtyard and RB.UIO.C1 modular configuration reduced the influence of urban conditions. Diversification analysis showed that for these four RBs, there are urban categories with lower predicted EUIs, though only 3.4% and 6.3% of their stock in clusters BCN.C1 and

UIO.C1 had lower values. The maximum decrements for the diversified RBs were 2.07 kWh/m² and 3.41 kWh/m² for Barcelona and Quito, respectively.

The final diversified energy demand was 15.96 MWh/year for 57 schools in Barcelona and 29.83 MWh/year for 214 schools in Quito. Table 8 shows the non-diversified and diversified energy demand for both stocks. Approaches differ significantly for clusters BCN.C1 and UIO.C1 as both RBs had EUIs similar to the lowest energy intensity in the diversified categories. In contrast, other RBs had EUIs equal to the average diversified energy intensity. The diversified approach increases the stocks' energy demand estimation by 5%. Nominal differences between methods are 651 MWh/year for Barcelona and 34 MWh/year for Quito. However, as RBs do not represent the entire educational stock in Barcelona, this difference could increase. To date, there is no available data on the final energy consumption of schools in Barcelona city; nevertheless, 2012 energy data for 212 schools in the coastal area for Barcelona province served for comparison [46]. On average, schools had an annual measured energy demand of 85 kWh/m². This value is slightly over-predicted (<1%) using this diversified approach, whereas the non-diversified method under-predicts it by 3%.

	Cluster	% Stock	Floor area [m ²]	Stock Energy Use		Delta
				Non-diversified Q _{ND} [MWh/year]	Diversified Q _D [MWh/year]	
BCN	BCN.C1	32.3	97236.1	7153.3	7712.6	-7.82%
	BCN.C2	29.43	88601.7	8163.3	8255.0	-1.12%
	Total	61.73	185837.8	15316.7	15967.7	-4.25%
UIO	UIO.C1	40.48	302480.3	10639.9	10802.9	-1.53%
	UIO.C2	59.52	439149.0	19161.4	19032.5	0.67%
	Total	100	741629.3	29801.3	29835.4	-0.11%

Table 8 Educational stock energy demand quantification

4. General discussion

The estimated EUI for the educational stock in Barcelona was 85.92 kWh/m²year and in Quito was 40.23 kWh/m²year. There are significant differences in EUIs between school typologies in each city, with the average EUI for BCN.C2 typology being 1.25 times higher than for BCN.C1. Similarly, EUI for UIO.C2 typology is 25% above UIO.C1. For Barcelona, the two validated

typologies only represent 61.73% of its educational stock and have an average EUI of 91.73 kWh/m²year. However, data suggests this section is the most energy-intensive, whereas the remaining 38.27% of this stock has an average EUI of 73.17 kWh/m²year (see Figure 4). RBs were more appropriate for Quito because of the stock homogeneity in construction practices and relatively simple envelopes. Therefore, two RBs represent this entire educational stock. The authors expected RB.UIO.C2 performed better than RB.UIO.C1 because of its lower thermal conductivity. RB.UIO.C1 low thermal mass allowed higher heat gains during occupancy hours and, therefore, its EUI was lower. However, the high thermal amplitude in RB.UIO.C1 requires careful consideration for the assessment of ECMs.

The motivation behind the simultaneous application of this bottom-up model in two very distinct educational stocks was the possibility to validate it against standard energy metrics for at least one stock [18,19]. Barcelona's conditioned stock was used as a control for the adequacy of this model, considering both stocks were assessed using the same segmentation, characterization, calibration and validation processes. While the authors do not expect that the prediction errors for both stocks to be the same, the UEM model provides a higher certainty in RBs selection for free-floating stocks. Also, the proposed validation at the building level permitted verifying that the RBs were representative of the average behaviour of the sample. Nevertheless, to confirm stocks' demand, large-scale field experimentation is required. Further effort should be placed on a building-by-building mapping and simulation for these stocks, as should be the inclusion of active equipment in the free-floating schools to measure their actual energy use and compared it to the hypothetical demand estimation.

This model characterization based on buildings' heat balance makes it transferable to all educational stocks alike. RBs should be accurate representations of their building stocks, but considering all variables would cause very complex and sometimes unrealistic RBs. Although the six variables used in this project proved sufficient for educational stock modelling – as suggested

previously in the literature [35] – higher variability stocks may require different and more numerous sets of classifiers for segmentation and characterization suited to their specificities [12,54]. Similarly, classifiers should adapt to the research end-goal; for example, for energy classification, COP and nominal power should be considered [20,32]. This on-demand segmentation capability provides flexibility to focus on specific aspects of the studied stocks. In addition, the reliance on statistical indexes to define accurate segmentation schemes eliminates the modeller's direct inference.

This diversification is a less resource-intensive method to account for the lost variability in reduced-domain stock modelling, whereas whole domain UEMs are computationally expensive [8]. The data-driven definition for the number of clusters and diversification categories produced highly representative categories, thus lowering the potential number of archetype buildings. This project's diversification focused on urban boundary modelling, but diversification could model stochastic occupancy and assess probabilistic characterizations [12,16]. Also, diversification could model primary energy use per fuel type and source contrary to average national data [31].

5. Conclusions

There is an array of available urban energy models that focus on the Global North, but scarce models for free-floating stocks because of the inability to validate their outcomes. Recognizing this difficulty in modelling free-floating building stocks, a novel reductive bottom-up model that relies on thermophysical building parameters was proposed and applied simultaneously in a conditioned stock and a free-floating stock. The designed two-step validation evaluated simultaneously the goodness-of-fit for the stock segmentation scheme and the appropriateness of the selected real-reference buildings to represent their stock at a building-by-building level. Also, this conditioned building stock was assessed using standard energy metrics to verify the

accuracy of this model. This verification showed errors below 1% for aggregated energy demand, thus confirming model adequacy. The main findings in this project are:

1. The annual energy demand for Barcelona educational stock was 15.96 MWh/year, and for Quito was 29.83 MWh/year. Their average energy use intensity was 85.92 kWh/m² and 40.23 kWh/m², respectively. However, it can increase up to 1.2 times because of urban boundaries.
2. Two reference schools only represent 61% of Barcelona educational stock because of edifices heterogeneity and retrofit interventions. However, the assessment of this stock in its as-is state allowed for proper segmentation and grouping of unforeseen similar buildings.
3. In Quito, 52% of its schools are modular steel-frame classrooms, and 48% are multi-storey concrete-frame buildings. Two reference buildings represent this entire stock because of standard construction practices and envelope materiality.
4. The proposed model has three stages: 1) K-means algorithm segments the stocks and identifies real-reference buildings, building-by-building energy data ratify this selection; 2) detailed Energy Plus models represent these reference buildings, and empirical data validate their outcomes; 3) joint probability distributions describe urban boundaries in the studied stocks, these boundaries inform RBs' EUI diversification.
5. Building-level validation and probability up-scaling increased the accuracy of aggregated energy demand predictions.
6. The additional effort for diversification is not justified to establish energy baselines because there is only a 5% variation between diversified and non-diversified approaches. However, diversification is better for building-level analyses, such as the assessment of energy conservation measures.

Future work will include the probabilistic modelling for reference buildings as will the propagation of uncertainty from building-level to urban-level energy estimation. Additional studies will assess energy conservation measures and green-envelope technologies to retrofit these stocks.

Acknowledgements: The authors would like to thank the local governments in Barcelona and Quito for the information they provided. Additional thanks to the schools' staff for their time and support and the Ecuadorian National Secretary of Higher Education, Science and Technology (SENESCYT) for awarding a research scholarship to Gabriela Ledesma (CZ02-000592-2018). This article is part of the first author's doctoral dissertation on optimizing a building's envelope individual surfaces through combinations of passive strategies.

Declarations of interest: none

APPENDIX A

Table A.1 Available reduced-domain urban energy models

Stock	Scale	Year	Model	Method	DATA		Aim	VALIDATION		SIMULATION		Ref
					Source	Type		Level	Metrics	Method	Tool	
W	NB	2017	Ph-A	Hierarchical clustering / K-mean	GIS data, technical codes	A	Identify reference buildings	AL / BL	Heating demand archetype and B-by-B	Steady-state	Python R language	[12]
R	NB	2018	Ph-A	K-mean / K-medoids	Field surveys / 3D reconstruction	M	Best clustering technique	AL	EUI archetype aggregated and B-by-B	Shoebox	UMI Rhino Matlab R language	[13]
E	N	2010	H	K-mean / PCA	Energy audits	M	Energy classification tool	SG	Silhouette function	None	Matlab	[14]
R	N	2012	H	Deterministic / Statistic	Database (energy use, geometry, thermal properties, occupancy) Database	M	Identify reference buildings	-	None	-	SPSS	[15]
R	CT	2017	Ph-M	Deterministic		A	Archetype calibration framework	AL / BL	NMBE, CvRMSE	Single-zone	Matlab	[16]
R	NB	2016	Ph-A	Hierarchical clustering / K-mean	Questionnaires	M	Validate reference building	BL	DH archetype and B-by-B	Dynamic	Design Builder Minitab Excel	[17]
R	NB	2017	Ph-M	Deterministic	Field surveys	M	Establish typologies	-	None	Detailed	Design Builder	[18]
R	N	2020	H	Deterministic / Statistic	National statistics	A	Establish typologies	-	None	-	R Language	[19]
R	N	2011	Ph-M	Deterministic	National statistics, Technical codes	A	Establish typologies	AL	EU archetype aggregated and national statistics	Quasi steady-state	TEE-KENAK	[20]
R	NB	2017	Ph-M	Deterministic	GIS	M	Identify reference buildings	-	None	Shoebox	Archsim	[21]
W	N	2011	Ph-M	Deterministic	National statistics, Technical codes	A	Identify reference buildings	AL	EU archetype aggregated and national statistics	Single-zone	Matlab	[22]
R	RG	2014	Ph-M	Deterministic	National statistics, Technical codes	A	Estimate energy savings	-	None	Quasi steady-state	Italian calculation method	[24]

E	N	2018	Ph-SA	Deterministic / K-means	Questionnaires	M	Establish typologies	-	None	Quasi steady-state	-	[31]
E	RG	2018	H	K-mean / Linear regression	EPC	M	Cost benefit energy retrofit to physical characteristics	AL	Index of determination	Dynamic	Matlab TRNSYS	[32]
E	RG	2015	H	K-mean / Linear regression	Official database	M	Best segmentation parameters	AL	EUI real vs regression model	None	-	[35]
C	N	2014	H	K-mean / Linear regression	Commercial Building Energy Database	A	Energy benchmark tool	AL	EUI cluster and energy star	-	-	[39]
W	N	2014	Ph-M	Deterministic	National statistics, Technical codes	A	Identify reference buildings	AL	EU archetype aggregated and national statistics	Single-zone	Matlab	[54]
R	RG	2011	H	Statistic / Hierarchical clustering	EPC	M	Compare deterministic and clustering	SG	Cophenetic coefficient	-	Matlab	[75]
R	N	2014	H	Deterministic & statistic	EPC, BBR	A	Estimate energy savings	AL	Heating demand archetype aggregated and national statistics	Quasi steady-state	Tabula calculation tool	[76]
R	RG	2014	H	Deterministic / Statistic	National statistics, Technical codes	A	Establish typologies	AL		-	-	[77]
E	RG	2014	Ph-A	K-means	Database (geometry, thermal properties and energy use)	M	Best segmentation parameters	SG	Regression coefficient	-	-	[78]
E	CT	2017	Ph-M	Deterministic	Field surveys / cadastral data	M	Identify reference buildings	-	None	-	-	[79]
C	N	2011	H	Deterministic / Statistic	ENEA project	A	Method for reference building	-	-	Dynamic	Design Builder	[80]
W	CT	2018	H	Deterministic / Statistic	EPC, National statistics	M	Identify reference buildings	BL	NRMSE of energy signature	Single-zone	R Language Design builder	[81]

STOCKS: Residential (R), Educational (E), Commercial (C), Whole stock (W). SCALE: Neighbourhood (NB), City (CT), Region (RG), National (N). MODEL TYPE: Physical with manual segmentation (Ph-M), Physical with semi-automated segmentation (Ph-SA), Physical with automated segmentation (Ph-A), hybrid (H). TYPE OF DATA: measured (M), estimated (A). VALIDATION LEVEL: aggregated (AL), building level (BL), segmentation validity (SG).

APPENDIX B

Table B.1 Monitored data in the reference school buildings

Category	Description	Method	Processing
Weather	Air temperature, humidity, global horizontal radiation, wind speed and direction, rain depth. Hourly records	City weather stations (closest to school location)	Irradiance components (MATLAB) Dew point (Magnus formula)
Indoor environment	Indoor air temperature and humidity. 15-minute records for a 3-month period in classrooms	Mini-dataloggers Error ± 0.5 °C $\pm 3\%$ RH	Weighted hour values Smooth of non-continuous data
Energy	Electricity and natural gas consumption for school year 2018-2019	Monthly bills	-
Operation	Occupancy densities and schedule Classrooms Offices/Halls/others	Questionnaires (teachers) Questionnaires (management)	Sub-hourly compact schedules
	Occupants behaviour (classrooms) Operation of windows and curtains Use of lighting systems Use of computation equipment Clothing	Questionnaires (teachers)	Sub-hourly compact schedules CLO insulation calculation from ASHRAE Fundamentals
	Setpoints Natural ventilation Heating Cooling	Questionnaires (management)	Interpolation operation schedules and measured indoor air temperature
Systems	HVAC type, location and service zone HVAC schedule Lighting type DHW type, service zone Ambient lighting use Lighting power Computing equipment specifications	Questionnaires (maintenance) Field surveys Field surveys	Sub-hourly compact schedules Lighting power density
Envelope	Thermal conductivity	Heat-flux meter	Average thermal conductivity
	In-site blueprints depicting current distribution, floor-to-ceiling heights, openable area of windows, location of active systems.	Architecture survey	2D digital line drawings (CAD)

Lighting power density was calculated as follows:

$$\text{For CFL} \quad LPD_{CFL} = \frac{L_p L_n BF N}{Area} \quad Eq. B.1$$

$$\text{For LED} \quad LPD_{LED} = \frac{\frac{L_p}{PF} N}{Area} \quad Eq. B.2$$

Where LPD_{CFL} is lighting power density for fluorescent luminaires, LPD_{LED} is lighting power density for LED luminaires, L_p is the lamp's nominal power, L_n is the number of lamps in a luminaire, BF is the ballast factor, N is the number of luminaires, and PF is the power factor.

APPENDIX C

Table C.1 Data description and sources used in the creation of the schools' datasets

Category	Description	Source	Ref
Identification	ID code	Official datasets	[62,63]
	Location		
	Contact information		
Form	Construction year	Cadastre	[82,83]
	Listings	Official datasets	[84,85]
	Renovation year	Project documents	[58–60]
	Renovation type and component	Project documents / field surveys	
	Gross floor area	Cadastre / GIS	
	Terrain area		
	Number of floors		
	Building Layout		
	Neighbouring		
	Orientation		
	Elevation		
Urban layout			
Envelope	Built density	GIS / field surveys	[58–60]
	Structure type	Blueprints /	[47,50]
	Wall materiality	Technical datasheets / field surveys /	
	Roof materiality	Technical codes	
	Fenestration type		
Systems	Electricity grid	Official datasets	[62,63]
	Heating		
	Cooling		
	DHW		
	Mechanical ventilation		
	Drinking water		
	Sewerage		
Operation	Schedule	Official datasets	[62,63]
	Number of students		
	Number of employees		
Domestic hot water (DHW), Geographic information systems (GIS).			

APPENDIX D. (K-mean clustering results)

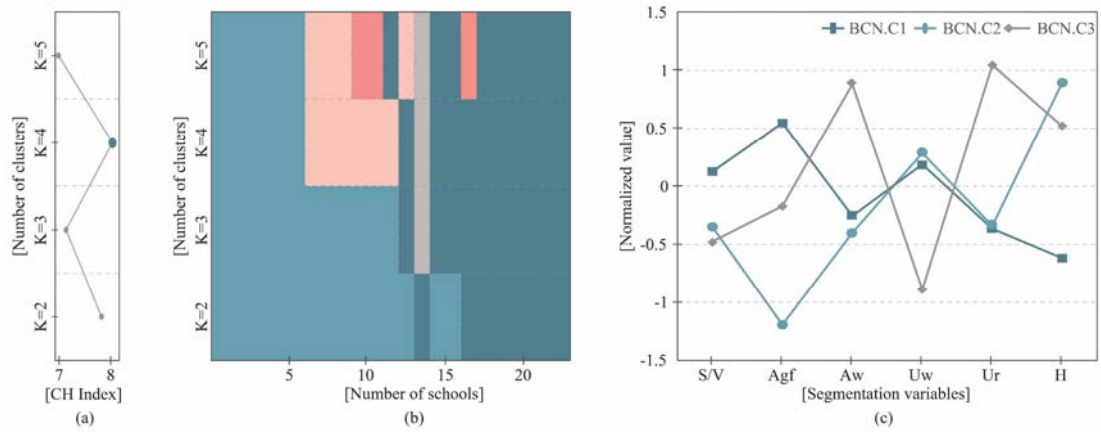


Figure D.1 Stock classification in Barcelona showing (a) Calinski-Harabasz index for different number of k clusters, (b) distribution of schools regarding number of clusters, and (c) standardized cluster centroids for $k = 4$

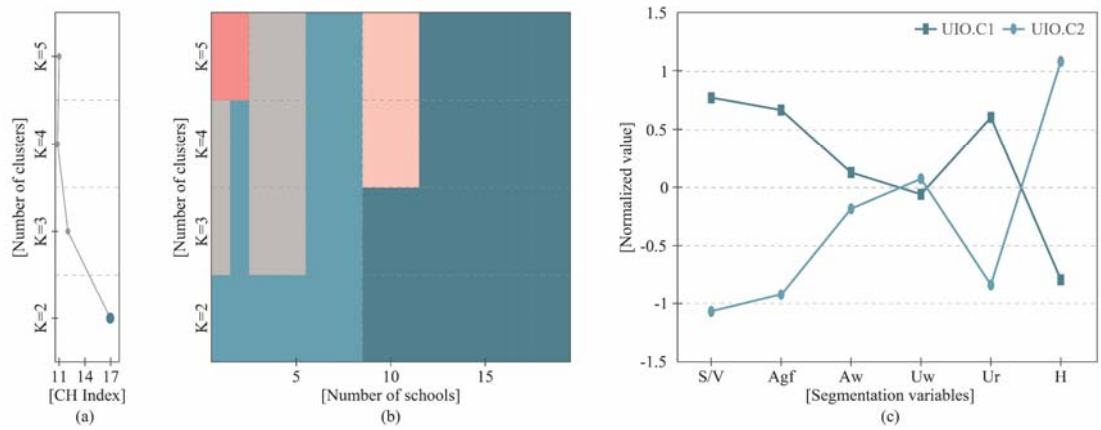


Figure D.2 Stock classification in Quito showing (a) Calinski-Harabasz index for different number of k clusters, (b) distribution of schools regarding number of clusters, and (c) standardized cluster centroids for $k = 2$

Table D.1 TESS and Silhouette indexes for the different clustering schemes

Index	Barcelona				Quito			
	K = 2	K = 3	K = 4	K = 5	K = 2	K = 3	K = 4	K = 5
TESS	96.05	76.55	58.13	47.98	54.03	43.11	34.17	26.05
Silhouette	0.207	0.225	0.270	0.257	0.414	0.289	0.257	0.281

APPENDIX E (Full descriptions for Reference School Buildings)

Reference School RB.BCN.C1

This school model represents 31 schools in Barcelona and 32.2% of the total building floor area. It is a three-story compact building distributed around a small central courtyard. The main façade is oriented due south-west and opens to a playground. This school is located in a low built-up density area with wide canyon streets on three of its sides - its low built-up density is due to the surrounding park and boulevard. This school complex also houses an independent gymnasium. This school has 22 classrooms and serves 375 students. This building was monitored from 3rd September to 10th December 2019 for indoor environmental parameters and during the last week of January 2020 for envelope thermal conductivity.

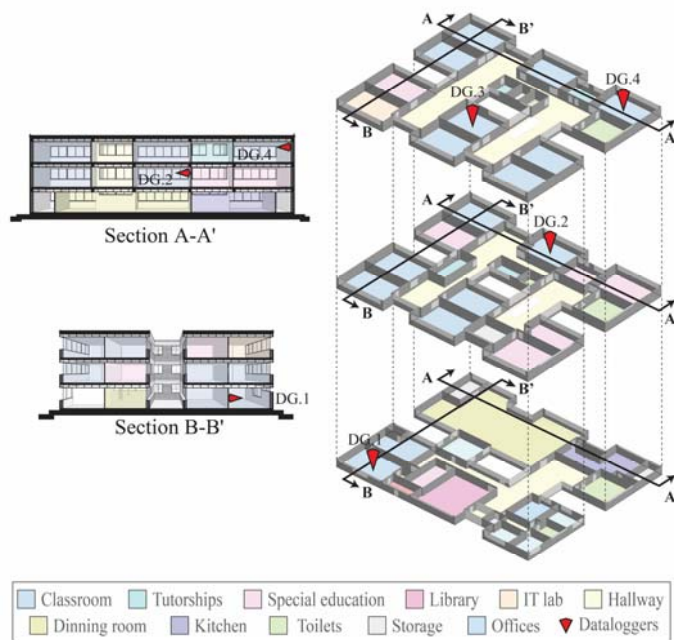


Figure E.1 Exploded axonometric for RB.BCN.C1 showing internal distribution and position of monitoring equipment

Table E.1 Internal gains per type of space in RB.BCN.C1

Space	Schedule	Occupancy [people/m ²]	Lighting Type	Lighting Power density [W/m ²]	Equipment [W/m ²]
Classrooms	9:00-11:00 11:30-12:30 15:00-16:30	0.5	FL	8.6	4.5
Offices	9:00-16:30	0.15	FL	6.0	15
Teachers rooms	9:00-16:30	0.15	FL	6.0	4.5
Dining room	12:30-15:00	0.2	FL	7.8	50 (kitchen)
Library	9:00-16:30	0.15	FL	7.2	3.5
Hall	8:30-18:00	0.05	FL	7.2	None
IT class	50% class schedule	0.5	FL	8.6	30

Table E.2 Thermal conductivity for envelope elements in RB.BCN.C1

Element	Material	Location	U-value [W/m ² K]	Thickness [m]	Heat capacity [kJ/m ² K]
External walls	280 mm brick, air cavity, 80 mm brick, 15 mm plaster	All	1.073	0.450	124.920
Ground floor	Ceramic tiles, 30 mm screed, 200 mm suspended concrete slab	All	1.791	0.250	221.000
	Vinyl floor covering, 40 mm screed, 200 mm suspended concrete slab	Classrooms, library	1.602	0.250	-
Roof	Ballast, 120 mm XPS, waterproofing, 75 mm screed, 300 mm concrete waffle slab, air cavity, 12.5 mm ceiling tiles	Top floor	0.226	1.050	10.500
	Waterproofing, 75 mm screed, 300 mm concrete waffle slab, 15 mm plaster	First floor	1.832	0.400	127.270
Floor / ceiling	Ceramic tiles, 30 mm screed, 300 mm concrete waffle slab, air cavity, 12.5 mm ceiling tiles	All	1.176	0.700	143.050
Party walls	15 mm plaster, 70 mm brick, 15 mm plaster	All	2.273	0.100	63.720
Windows	6 mm single clear glazing in aluminium frames	All	5.770	0.003	
Door	Hardwood	All	2.774	0.040	22.400

Conductivity of construction materials or assemblies retrieved from [50]

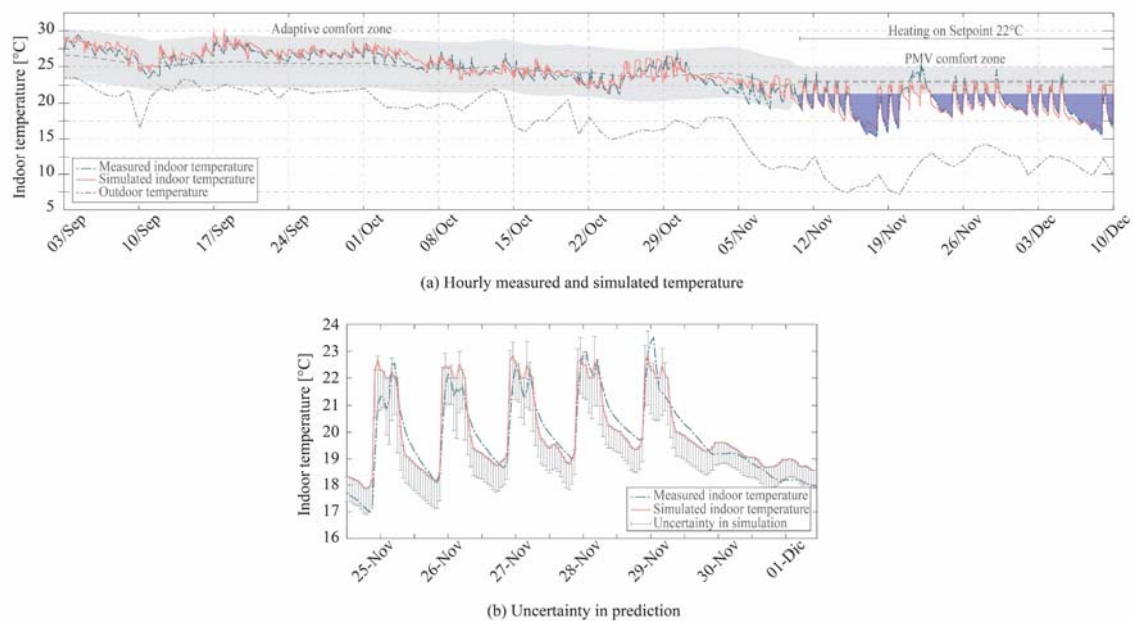


Figure E.2 Calibration and uncertainty in model prediction for indoor air temperature in RB.BCN.C1

Reference School RB.BCN.C2

This typology represents 26 schools in Barcelona and accounts for 29.43% of this stock total floor area. It has two multi-storey parallel blocks with three storeys in the front block and four storeys in the rear. The front block is oriented southward to an open courtyard, while the rear block faces a multi-story residential building. This school is located in a medium built-up density area with narrow canyon streets on two sides and a park located on its entrance side. This school has 18 classrooms and serves 250 students. This building was monitored from 2nd September to 11th December 2019 for indoor environmental parameters and during the third

week in January 2020 for envelope thermal conductivity.

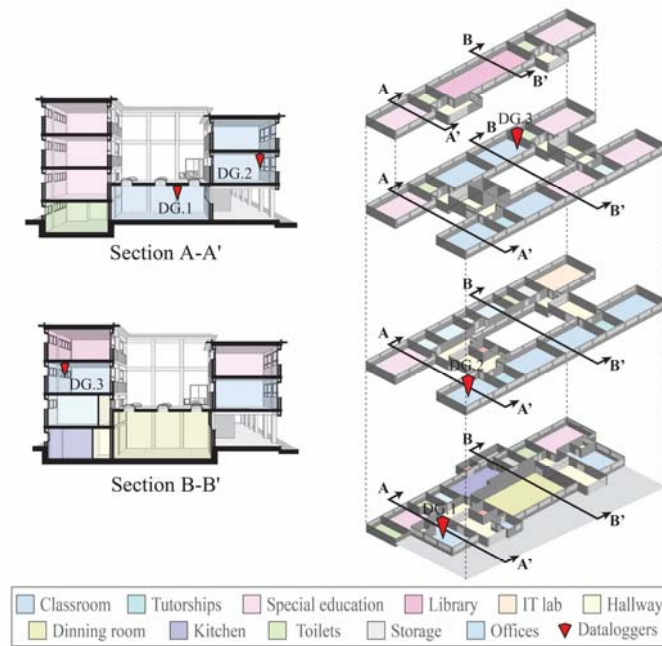


Figure E.3 Exploded axonometric for RB.BCN.C2 showing internal distribution and position of monitoring equipment. Dataloggers (DG).

Table E.3 Internal gains per type of space in RB.BCN.C2

	Schedule	Occupancy [people/m2]	Lighting Type	Lighting Power density [W/m2]	Equipment [W/m2]
Classrooms	9:00-11:00	0.5	FL	8.6	4.5
	11:30-12:30				
	15:00-16:30				
Offices	9:00-16:30	0.15	FL	5.0	15
Teachers rooms	9:00-16:30	0.15	FL	7.6	4.5
Dining room	12:30-15:00	0.2	FL	6.6	50 (kitchen)
Library	9:00-16:30	0.15	FL	7.3	3.5
Hall	8:30-18:00	0.05	FL	3.0	None
IT class	50% class schedule	0.5	FL	8.6	30

Table E.4 Thermal conductivity for envelope elements in RB.BCN.C2

Element	Material	Location	U-value [W/m ² K]	Thickness [m]	Heat capacity [kJ/m ² K]
External walls	130 mm brick, air cavity, 80 mm hollow double brick, 15 mm plaster	Front and rear facades	1.328	0.300	131.720
	20 mm plaster, 130 mm brick, air cavity, 80 mm hollow double brick, 15 mm plaster	East and west facades	1.269	0.300	131.720
	130 mm concrete cast, air cavity, 80 mm hollow double brick, 15 mm plaster	Below grade, rear façade	1.622	0.300	131.720
Ground floor	Ceramic tiles, 30 mm screed, 150 mm concrete slab, gravel, PE film	All	2.558	0.300	226.000

Roof	Vinyl floor covering, 30 mm screed, 150 mm concrete slab, gravel, PE film	Ground floor classrooms	2.496	0.300	225.800
	Clay tiles, 40 mm cement plaster, waterproofing, 75 mm screed, 60 mm XPS, 250 mm concrete waffle slab, 15 mm internal rendering	Top floor	0.388	0.500	127.700
	Waterproof roof covering, 60 mm XPS, 75mm screed, 250 mm concrete waffle slab, 15 mm plaster	First floor	0.396	0.400	127.700
Floor / ceiling	Ceramic tiles, 30 mm screed, 250 mm concrete waffle slab, 15 mm internal rendering	All	1.697	0.300	143.400
Party walls	15 mm plaster, 70 mm brick, 15 mm plaster	All	2.273	0.100	63.720
Windows	6 mm single clear glazing in aluminium frames	All	5.770	0.003	
Door	Hardwood	All	2.774	0.040	22.400

Conductivity of construction materials or assemblies retrieved from [50]

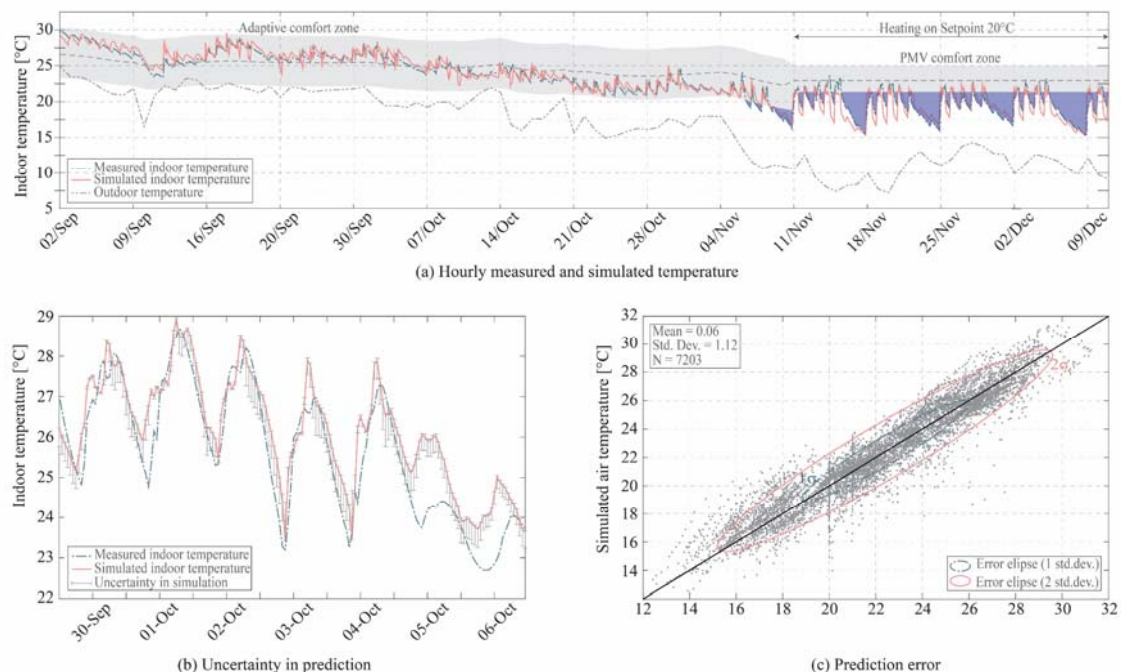


Figure E.4 Calibration and uncertainty in model prediction for indoor air temperature in RB.BCN.C2

Reference School RB.UIO.C1

This model is the most common in Quito and represents 112 schools. It is composed of lightweight steel-frame modular classrooms. However, this model accounts for only 40.48% of the stocks area because of its small floor area. The modules can house one to floor classrooms that are accessible from the exterior. This reference school has a cross-shape distribution, occupies a large terrain, and locates in a low-density urban area. This schools plot limits with streets on three sides and low-rise residential buildings on its fourth side. This reference school has 16 classrooms and serves 638 students. The building complex includes a two-story independent building functioning as a first-aid centre. Classrooms were monitored from 3rd April 3rd to 2nd July 2019. All building blocks are free-floating, do not have domestic hot water nor mechanical ventilation. There is a small kitchen in an independent shed.

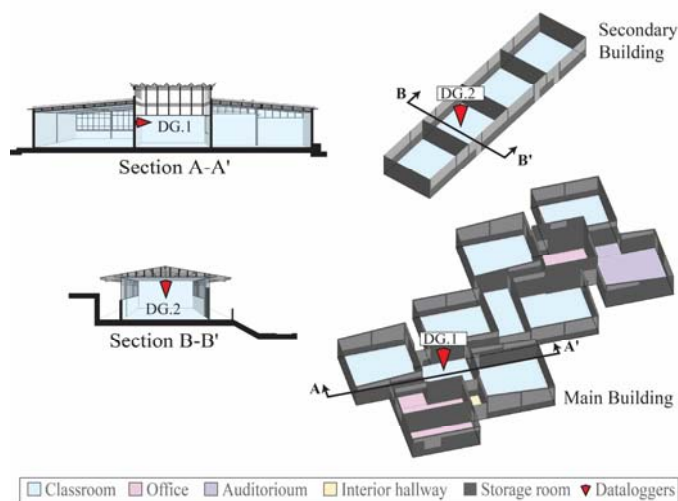


Figure E.5 Axonometric for RB.UIO.C1 showing internal distribution and position of monitoring equipment. Dataloggers (DG).

Table E.5 Internal gains per type of space in RB.UIO.C1

Space	Location	Schedule	Unit Area [m ²]	Occupancy [people/m ²]	Lighting Type	Lighting Power density [W/m ²]	Equipment [W/m ²]
Classrooms	SB	7:15-9:15	37.3	0.95	LED	3.85	None
	MB	9:45-12:35	30.6	0.80	LED	7.05	None
	MB		53.3	0.65	FLC	2.25	None
Offices		7:00-13:30		0.15	FLC	4.10	10
Auditorium		2 hours per week		1.4	FLC	2.25	10
Waiting room		7:00-13:30		0.2	FLC	2.8	None

Table E.6 Thermal conductivity for envelope elements in RB.UIO.C1

Element	Material	Location	U-value	Thickness	Heat capacity
			[W/m ² K]	[m]	[kJ/m ² K]
External walls	150 mm medium weight concrete block, 20 mm dense plaster	SB	1.973	0.190	105.500
	130 mm solid brick, 20 mm dense plaster	MB	2.279	0.170	158.590
	Ceramic tiles, 30 mm screed, 100 mm cast concrete, gravel, PE film	SB, Admin	2.505	0.240	152.690
Ground floor	19 mm timber, 10 mm screed, 100 mm cast concrete, gravel, PE film	Classrooms MB	2.375	0.230	159.320
	10 mm carpet, 30 mm screed, 100 mm cast concrete, gravel, PE film	Principal office	2.331	0.240	-
	6 mm asbestos-cement sheet on 250 mm concrete joists, 12.5 mm plasterboard ceiling between joists	MB	2.157	0.220	-
Roof	6 mm asbestos-cement sheet on 150 mm steel joists	SB	6.452	0.006	4.560
	4 mm zinc sheet on 100 mm steel joists, 12.5 mm plasterboard ceiling	Between blocks MB	2.352	0.120	-
	30 mm screed, 150 mm cast concrete, 13 mm dense plaster	MB	3.696	0.180	234.000

Ceiling	12.5 mm plasterboard ceiling	All	3.790	0.015	2.850
Party walls	150 mm medium weight concrete block, 13 mm dense plaster	SB	1.863	0.180	96.430
	130 mm solid brick, 13 mm dense plaster	MB	1.891	0.160	158.590
Windows	3 mm single clear glazing in iron cast frames	All	5.894	0.003	
Door	Hardwood	MB	2.557	0.040	35.130
	Steel sheet on iron frame	SB	3.124	0.003	11.920

Conductivity of construction materials or assemblies retrieved from [47]

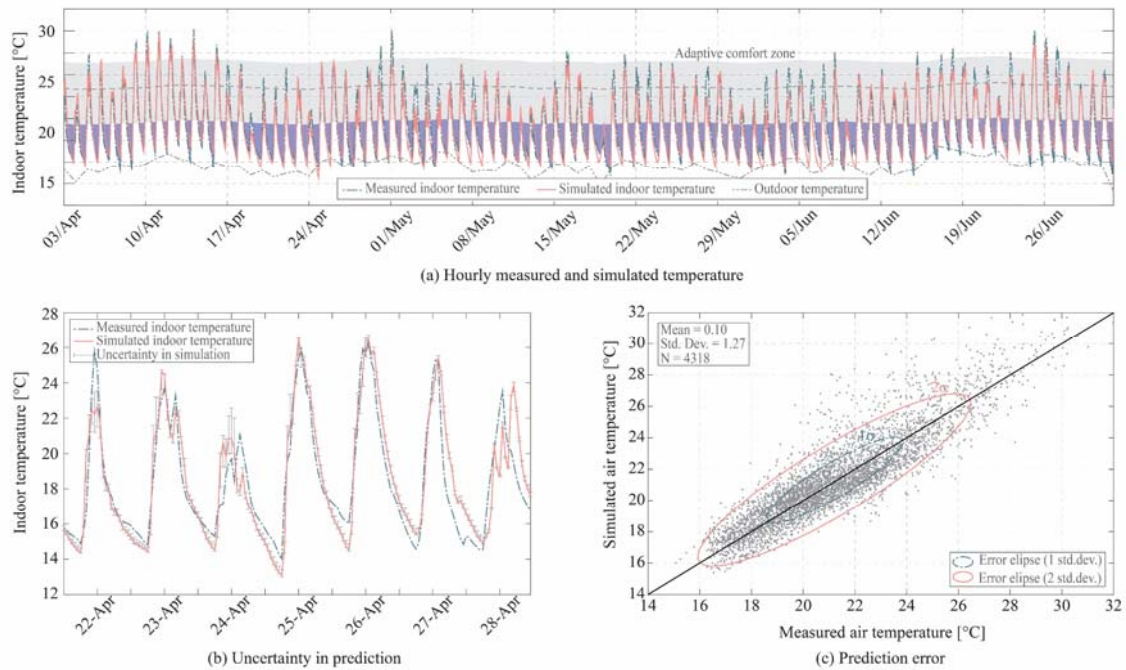


Figure E.6 Calibration and uncertainty in model prediction for indoor air temperature in RB.UIO.C1

Reference School RB.UIO.C2

This building model groups 102 schools in Quito and 59.52% of the stock's area. This model has larger floor areas than the modular typology, and some buildings surpass the 10000 m². Large schools usually have several independent buildings belonging to this typology. This reference school is a two-story L-shaped building open to a central courtyard. All circulations are external and only covered by the roof slab. This building has a concrete frame structure and waffle slabs. This school has no construction setbacks and shares a party wall. Its main façade (entrance) is oriented due northeast, has 14 classrooms, and serves 631 students. This school complex also houses two modular units with similar characteristics as those in RB.UIO.C1. This building was monitored from 4th April to 2nd July 2019. It is also free-floating, lacks domestic hot water and mechanical ventilation. A small independent shed serves as a kitchen.

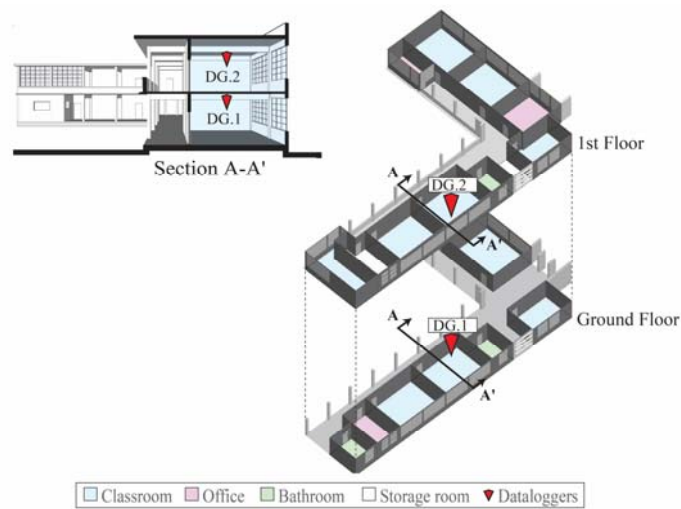


Figure E.7 Exploded axonometric for RB.UIO.C2 showing internal distribution and position of monitoring equipment. Dataloggers (DG)

Table E.7 Internal gains per type of space in RB.UIO.C2

Space	Location	Schedule	Occupancy [people/m ²]	Lighting Type	Lighting Power density [W/m ²]	Equipment [W/m ²]
Classrooms	PB	7:15-10:15	0.55	LED	2.25	None
		10:45-12:35				
	PA	7:15-10:15	0.65	LED	2.25	None
		10:45-12:35				
Offices		13:15-16:15	0.85			
Toilets		16:45-18:35				
		7:00-16:00	0.1	LED	1.50	10
		7:00-18:45	0.05	FLC	1.2	None

Table E.8 Thermal conductivity for envelope elements in RB.UIO.C2

Element	Material	Location	U-value [W/m ² K]	Thickness [m]	Heat capacity [kJ/m ² K]
External walls	200 mm medium weight concrete block, 20 mm dense plaster	All	1.814	0.240	99.450
Ground floor	Ceramic tiles, 30 mm screed, 100 mm cast concrete, gravel, PE film	All	3.045	0.240	238.580
Roof	60 mm screed, 200 mm reticular concrete slab, 13 mm dense plaster	All	2.310	0.270	230.780
Floor / ceiling	19 mm timber, 20 mm screed, 100 mm concrete slab, 13 mm dense plaster	All	2.150	0.150	218.960
Party walls	200 mm medium weight concrete block, 20 mm dense plaster	All	1.559	0.240	99.450
Windows	3 mm single clear glazing in iron cast frames	All	5.894	0.003	
Door	Hardwood	All	2.557	0.040	35.130

Conductivity of construction materials or assemblies retrieved from [47]

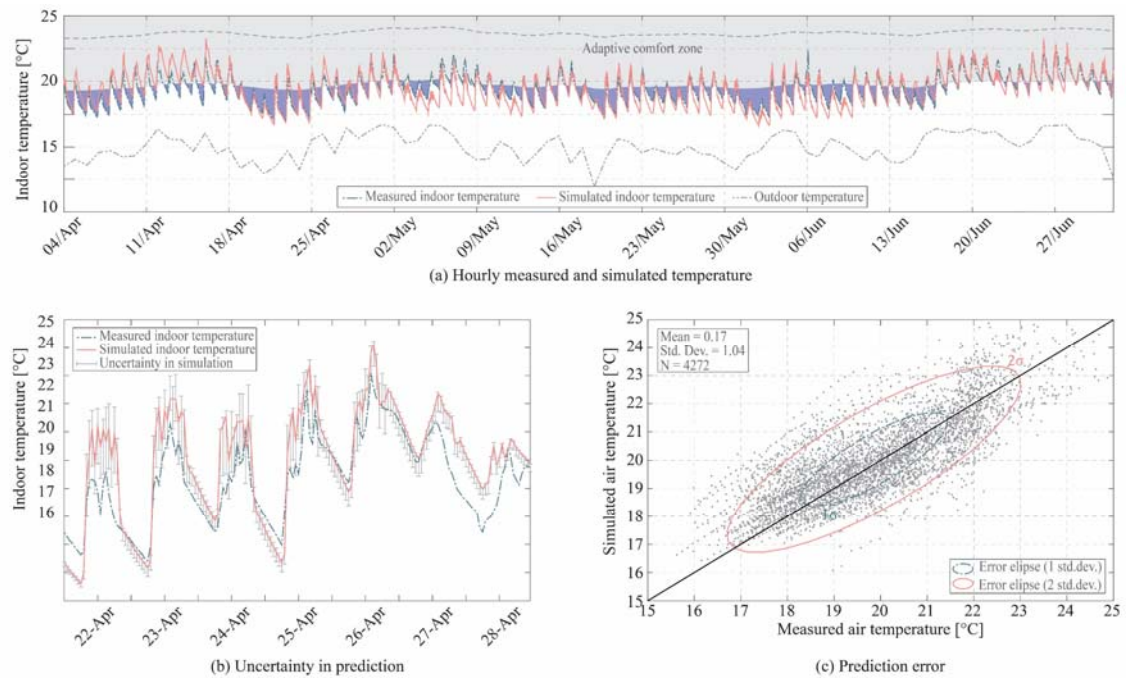


Figure E.8 Calibration and uncertainty in model prediction for indoor air temperature in RB.UIO.C2

References

- [1] International Energy Agency, Technology Roadmap. Energy efficient building envelopes, Paris, France, 2013.
- [2] F. Ascione, N. Bianco, R.F. De Masi, G.M. Mauro, G.P. Vanoli, Energy retrofit of educational buildings: Transient energy simulations, model calibration and multi-objective optimization towards nearly zero-energy performance, *Energy Build.* 144 (2017) 303–319. <https://doi.org/10.1016/j.enbuild.2017.03.056>.
- [3] M. Rabani, H.B. Madessa, N. Nord, A state-of-art review of retrofit interventions in buildings towards nearly zero energy level, *Energy Procedia.* 134 (2017) 317–326. <https://doi.org/10.1016/j.egypro.2017.09.534>.
- [4] L.G. Swan, V.I. Ugursal, Modeling of end-use energy consumption in the residential sector: A review of modeling techniques, *Renew. Sustain. Energy Rev.* 13 (2009) 1819–1835. <https://doi.org/10.1016/j.rser.2008.09.033>.
- [5] A. Sola, C. Corchero, J. Salom, M. Sanmarti, Multi-domain urban-scale energy modelling tools: A review, *Sustain. Cities Soc.* 54 (2020) 101872. <https://doi.org/10.1016/j.scs.2019.101872>.
- [6] T. Hong, Y. Chen, X. Luo, N. Luo, S.H. Lee, Ten questions on urban building energy modeling, *Build. Environ.* 168 (2020) 106508. <https://doi.org/10.1016/j.buildenv.2019.106508>.
- [7] M. Brøgger, K.B. Wittchen, Estimating the energy-saving potential in national building stocks – A methodology review, *Renew. Sustain. Energy Rev.* 82 (2018) 1489–1496. <https://doi.org/10.1016/j.rser.2017.05.239>.
- [8] C. Cerezo Davila, C.F. Reinhart, J.L. Bemis, Modeling Boston: A workflow for the efficient generation and maintenance of urban building energy models from existing geospatial datasets, *Energy.* 117 (2016) 237–250. <https://doi.org/10.1016/j.energy.2016.10.057>.
- [9] T. (LBNL) Hong, Y. (LBNL) Chen, S.H. (LBNL) Lee, M.P. (LBNL) Piette, Y. (LBNL) Chen, M.P. (LBNL) Piette, CityBES: A web-

- based platform to support city-scale building energy efficiency, 5th Int. Urban Comput. Work. San Fr. (2016) 10.
- [10] M. Deru, K. Field, D. Studer, K. Benne, B. Griffith, P. Torcellini, B. Liu, M. Halverson, D. Winiarski, M. Rosenberg, M. Yazdani, J. Huang, D. Crawley, U.S. Department of Energy commercial reference building models of the national building stock, National Renewable Energy Laboratory, 2011. http://digitalscholarship.unlv.edu/renew_pubs/44.
 - [11] I.P. Tabula, National Building Typologies, 2012. (n.d.). <http://episcopo.eu/building-typology/overview/> (accessed April 2, 2019).
 - [12] N. Ghiassi, A. Mahdavi, Reductive bottom-up urban energy computing supported by multivariate cluster analysis, *Energy Build.* 144 (2017) 372–386. <https://doi.org/10.1016/j.enbuild.2017.03.004>.
 - [13] X. Li, R. Yao, M. Liu, V. Costanzo, W. Yu, W. Wang, A. Short, B. Li, Developing urban residential reference buildings using clustering analysis of satellite images, *Energy Build.* 169 (2018) 417–429. <https://doi.org/10.1016/j.enbuild.2018.03.064>.
 - [14] N. Gaitani, C. Lehmann, M. Santamouris, G. Mihalakakou, P. Patargias, Using principal component and cluster analysis in the heating evaluation of the school building sector, *Appl. Energy*. 87 (2010) 2079–2086. <https://doi.org/10.1016/j.apenergy.2009.12.007>.
 - [15] A.A. Famuyibo, A. Duffy, P. Strachan, Developing archetypes for domestic dwellings - An Irish case study, *Energy Build.* 50 (2012) 150–157. <https://doi.org/10.1016/j.enbuild.2012.03.033>.
 - [16] M.H. Kristensen, R.E. Hedegaard, S. Petersen, Hierarchical calibration of archetypes for urban building energy modeling, *Energy Build.* 175 (2018) 219–234. <https://doi.org/10.1016/j.enbuild.2018.07.030>.
 - [17] A. Schaefer, E. Ghisi, Method for obtaining reference buildings, *Energy Build.* 128 (2016) 660–672. <https://doi.org/10.1016/j.enbuild.2016.07.001>.
 - [18] R.J. Muringathuparambil, J.K. Musango, A.C. Brent, P. Currie, Developing building typologies to examine energy efficiency in representative low cost buildings in Cape Town townships, *Sustain. Cities Soc.* 33 (2017) 1–17. <https://doi.org/10.1016/j.scs.2017.05.011>.
 - [19] C. Molina, M. Kent, I. Hall, B. Jones, A data analysis of the Chilean housing stock and the development of modelling archetypes, *Energy Build.* 206 (2020). <https://doi.org/10.1016/j.enbuild.2019.109568>.
 - [20] E.G. Dascalaki, K.G. Droutsas, C.A. Balaras, S. Kontoyiannidis, Building typologies as a tool for assessing the energy performance of residential buildings - A case study for the Hellenic building stock, *Energy Build.* 43 (2011) 3400–3409. <https://doi.org/10.1016/j.enbuild.2011.09.002>.
 - [21] C.S. Monteiro, A. Pina, C. Cerezo, C. Reinhart, P. Ferrão, The Use of Multi-detail Building Archetypes in Urban Energy Modelling, *Energy Procedia*. 111 (2017) 817–825. <https://doi.org/10.1016/j.egypro.2017.03.244>.
 - [22] G. Medina Benejam, É. Mata, A.S. Kalagasidis, F. Johnsson, Bottom-up characterization of the Spanish building stock for energy assessment and model validation, in: *Retrofit 2012*, Manchester, UK, 2012: p. 10. <http://publications.lib.chalmers.se/records/fulltext/164499.pdf>.
 - [23] C.F. Reinhart, C. Cerezo Davila, Urban building energy modeling - A review of a nascent field, *Build. Environ.* 97 (2016) 196–202. <https://doi.org/10.1016/j.buildenv.2015.12.001>.
 - [24] I. Ballarini, S.P. Corgnati, V. Corrado, Use of reference buildings to assess the energy saving potentials of the residential building stock: The experience of TABULA project, *Energy Policy*. 68 (2014) 273–284.

- <https://doi.org/10.1016/j.enpol.2014.01.027>.
- [25] T. Loga, B. Stein, N. Diefenbach, TABULA building typologies in 20 European countries—Making energy-related features of residential building stocks comparable, *Energy Build.* 132 (2016) 4–12. <https://doi.org/10.1016/j.enbuild.2016.06.094>.
 - [26] M. Kavgic, A. Mavrogianni, D. Mumovic, A. Summerfield, Z. Stevanovic, M. Djurovic-Petrovic, A review of bottom-up building stock models for energy consumption in the residential sector, *Build. Environ.* 45 (2010) 1683–1697. <https://doi.org/10.1016/j.buildenv.2010.01.021>.
 - [27] D. Österreicher, S. Geissler, Refurbishment in Educational Buildings - Methodological Approach for High Performance Integrated School Refurbishment Actions, *Energy Procedia.* 96 (2016) 375–385. <https://doi.org/10.1016/j.egypro.2016.09.163>.
 - [28] J.S. Carlos, H. Corvacho, Retrofit measures in old elementary school buildings towards energy efficiency, *J. Civ. Eng. Manag.* 16 (2010) 567–576. <https://doi.org/10.3846/jcem.2010.63>.
 - [29] C. Calice, C. Clemente, L. de Santoli, F. Fraticelli, Guidelines for the retrofit of the school building stock for sustainable urban regeneration of the city of Rome, *WIT Trans. Ecol. Environ.* 155 (2011) 417–428. <https://doi.org/10.2495/SC120351>.
 - [30] D. D’Agostino, L. Daraio, C. Marino, F. Minichiello, Cost-optimal methodology and passive strategies for building energy efficiency: a case-study, *Archit. Sci. Rev.* 0 (2018) 1–10. <https://doi.org/10.1080/00038628.2018.1491826>.
 - [31] University of Belgrade, National Typology of School Buildings in Serbia, Belgrade, 2018. <http://eeplatforma.arh.bg.ac.rs/publikacije?tab=0>.
 - [32] P. Marrone, P. Gori, F. Asdrubali, L. Evangelisti, L. Calcagnini, G. Grazieschi, Energy benchmarking in educational buildings through cluster analysis of energy retrofitting, *Energies.* 11 (2018) 1–20. <https://doi.org/10.3390/en11030649>.
 - [33] G. Ledesma, J. Nikolic, O. Pons-Valladares, Bottom-up model for the sustainability assessment of rooftop-farming technologies potential in schools in Quito, Ecuador, *J. Clean. Prod.* 274 (2020) 122993. <https://doi.org/10.1016/j.jclepro.2020.122993>.
 - [34] C. Jie, Review on the Research of K-means Clustering Algorithm in Big Data, 2020 IEEE 3rd Int. Conf. Electron. Commun. Eng. (ICECE), *Electron. Commun. Eng. (ICECE)*, 2020 IEEE 3rd Int. Conf. (2020) 107. <http://mendeley.csuc.cat/fitxers/199cfa1942914869ac73399a82a4d02e> (accessed February 26, 2021).
 - [35] R. Arambula Lara, G. Pernigotto, F. Cappelletti, P. Romagnoni, A. Gasparella, Energy audit of schools by means of cluster analysis, *Energy Build.* 95 (2015) 160–171. <https://doi.org/10.1016/j.enbuild.2015.03.036>.
 - [36] ISO, ISO 13370:2017 Thermal performance of buildings - Heat transfer via the ground - Calculation methods, 3rd ed., 2017.
 - [37] ISO, ISO 6946:2017 Building components and building elements - Thermal resistance and thermal transmittance - Calculation methods, 3rd ed., 2017.
 - [38] C. Cerezo, J. Sokol, S. AlKhaled, C. Reinhart, A. Al-Mumin, A. Hajiah, Comparison of four building archetype characterization methods in urban building energy modeling (UBEM): A residential case study in Kuwait City, *Energy Build.* 154 (2017) 321–334. <https://doi.org/10.1016/j.enbuild.2017.08.029>.
 - [39] X. Gao, A. Malkawi, A new methodology for building energy performance benchmarking: An approach based on

- intelligent clustering algorithm, *Energy Build.* 84 (2014) 607–616. <https://doi.org/10.1016/j.enbuild.2014.08.030>.
- [40] M. Charrad, N. Ghazzali, V. Boiteau, A. Niknafs, Nbclust: An R package for determining the relevant number of clusters in a data set, *J. Stat. Softw.* 61 (2014) 1–36. <https://doi.org/10.18637/jss.v061.i06>.
- [41] European Committee for Standardization, *Energy performance of buildings - Ventilation for buildings - Part 1: Indoor environmental input parameters for design and assessment of energy performance of buildings addressing indoor air quality, thermal environment, lighting and acoustics - Module M1*, 2019.
- [42] R. and A.C.E. American Society of Heating, *ANSI/ASHRAE Standard 55-2013: Thermal Environmental Conditions for Human Occupancy*, Atlanta, 2013.
- [43] É. Mata, A.S. Kalagasidis, F. Johnsson, A modelling strategy for energy, carbon, and cost assessments of building stocks, *Energy Build.* 56 (2013) 100–108. <https://doi.org/10.1016/j.enbuild.2012.09.037>.
- [44] Lawrence Berkeley National Laboratory, *THERM. Windows & Daylighting. Building Technology and Urban Systems*, (n.d.). <https://windows.lbl.gov/software/therm> (accessed March 2, 2021).
- [45] J.S. Stein, W.F. Holmgren, J. Forbess, C.W. Hansen, PVLIB : Open Source Photovoltaic Performance Modeling Functions for Matlab and Python, in: 2016 IEEE 43rd Photovolt. Spec. Conf., IEEE, Portland, OR, USA, 2016: pp. 3425–3430. <https://doi.org/10.1109/PVSC.2016.7750303>.
- [46] B. Pujol G., M. Wassouf, *Estudi de rehabilitació energètica amb criteris nzeb d'edificis d'equipaments públics municipals*, 2015.
- [47] Ministerio de Desarrollo Urbano y Vivienda, *Eficiencia Energética en Edificaciones Residenciales*, MIDUVI, Registro Oficial, Año I, Edición Especial No. 358, Ecuador, 2018. <https://www.habitatyvivienda.gob.ec/documentos-normativos-nec-norma-ecuatoriana-de-la-construccion/>.
- [48] Ministerio de Fomento (España), *Documento Básico HE Ahorro de Energía*, 2019. <http://www.arquitectura-tecnica.com/hit/Hit2016-2/DBHE.pdf>.
- [49] CIBSE, *CIBSE Guide A: Environmental Design*, 2015. www.cibse.org.
- [50] Ministerio de Vivienda de España, *Catálogo de Elementos Constructivos del CTE*, 2011. <http://itec.cat/cec/>.
- [51] ISO, *ISO 10456:2007 Building materials and products - Hygrothermal properties - Tabulated design values and procedures for determining declared and design thermal values*, 3rd ed., 2007.
- [52] G. Havenith, Metabolic rate and clothing insulation data of children and adolescents during various school activities, *Ergonomics*. 50 (2007) 1689–1701. <https://doi.org/10.1080/00140130701587574>.
- [53] M. Royapoor, T. Roskilly, Building model calibration using energy and environmental data, *Energy Build.* 94 (2015) 109–120. <https://doi.org/10.1016/j.enbuild.2015.02.050>.
- [54] É. Mata, A. Sasic Kalagasidis, F. Johnsson, Building-stock aggregation through archetype buildings: France, Germany, Spain and the UK, *Build. Environ.* 81 (2014) 270–282. <https://doi.org/10.1016/j.buildenv.2014.06.013>.
- [55] R. and A.C.E. American Society of Heating, *ASHRAE Guideline: Measurement of Energy and Demand Savings*, Atlanta, USA, 2002.
- [56] F. Roberti, U.F. Oberegger, A. Gasparella, Calibrating historic building energy models to hourly indoor air and surface temperatures: Methodology and case study, *Energy Build.* 108 (2015) 236–243.

<https://doi.org/10.1016/j.enbuild.2015.09.010>.

- [57] National Renewable Energy Laboratory, Weather Data, (n.d.). <https://www.energyplus.net/weather> (accessed February 23, 2021).
- [58] A. de Barcelona, Geoportal BCN, (n.d.). <http://w133.bcn.cat/geoportalbcn/GeoPortal.aspx?lang=es> (accessed March 2, 2021).
- [59] Secretaria General de Planificaci3n del Municipio del Distrito Metropolitano de Quito, GEOPORTAL - Gobierno Abierto Quito, (n.d.). http://gobiernoabierto.quito.gob.ec/?page_id=1114 (accessed March 2, 2021).
- [60] Secretaria General de Planificaci3n del Municipio del Distrito Metropolitano de Quito, INFORMACI3N GEOGRÁFICA - Gobierno Abierto Quito, (n.d.). http://gobiernoabierto.quito.gob.ec/?page_id=1122 (accessed March 2, 2021).
- [61] G. Ledesma, J. Nikolic, O. Pons-Valladares, Towards a More Energy Efficient Educational Architecture in Cities: Typologies of Barcelona and Quito Public Schools for Energy Modelling, in: CPSV (Ed.), XIII CTV 2019 Proc. XIII Int. Conf. Virtual City Territ. "Challenges Paradig. Contemp. City", UPC, Barcelona, Spain, 2019: p. 14. <https://doi.org/10.5821/ctv.8505>.
- [62] Ajuntament de Barcelona, Enseñanza secundaria. Centros y profesores. Cursos 2013-2017, (2017). <http://www.bcn.cat/estadistica/castella/dades/anuari/cap05/C0502060.htm> (accessed November 8, 2018).
- [63] Ministerio de Educaci3n del Ecuador, AMIE (Estadísticas educativas a partir de 2009-2010), 2009. (2018). <https://educacion.gob.ec/amie/> (accessed November 13, 2018).
- [64] Ministerio de Educaci3n del Ecuador, Acuerdo Nro. MINEDUC-MINEDUC-2018-00087-A Programa Nacional de Infraestructura y Gesti3n Educativa - Mi aula al 100%, Quito, Ecuador, 2018.
- [65] G. Llad3, D. Guerrero, A. Romero, Model metropolità d'escoles NZEB - Àrea Metropolitana de Barcelona, Area Metrop. Barcelona. (2015). https://www.amb.cat/es/web/ecologia/sostenibilitat/transicio-energetica/projectes/detall/-/projecteobert/model-metropolita-d-escoles-nzeb/5848153/11818?_ProjecteObertSearchListPortlet_WAR_AMBSearchPortletportlet_pageNum=1&_ProjecteObertSearchListPortlet_W (accessed February 10, 2021).
- [66] Escuela Politécnica Nacional, Proyecto de seguridad sísmica para las construcciones escolares. Invirtiendo en el futuro de Quito., Stanford: GeoHazards Internation, Quito, Ecuador, 1995.
- [67] G. Ledesma, N. Hamza, Assessment of thermal comfort and passive design strategies in Millennium Schools in Ecuador, PLEA Conf. Proc. Des. to Thrive. I (2017) 764–771.
- [68] US Department of Energy, Building Energy-Efficient Schools in New Orleans Lessons Learned n n Langston Hughes Elementary School, New Orleans, 2005.
- [69] H. Erhorn, H. Erhom-Kluttig, J. Reiß, Plus energy schools in Germany - Pilot projects and key technologies, Energy Procedia. 78 (2015) 3336–3341. <https://doi.org/10.1016/j.egypro.2015.11.747>.
- [70] N. Gaitani, L. Cases, E. Mastrapostoli, E. Eliopoulou, Paving the way to nearly zero energy schools in Mediterranean region-ZEMedS project, Energy Procedia. 78 (2015) 3348–3353. <https://doi.org/10.1016/j.egypro.2015.11.749>.
- [71] EURECAT, Energy simulations results for case studies nZEB renovations, 2016.
- [72] H. Erhorn-Kluttig, H. Erhorn, School of the Future - Towards zero emission with high performance indoor environment, Energy Procedia. 48 (2014) 1468–1473. <https://doi.org/10.1016/j.egypro.2014.02.166>.

- [73] U. Berardi, M. Manca, P. Casaldaliga, F. Pich-Aguilera, From high-energy demands to nZEB: The retrofit of a school in Catalonia, Spain, *Energy Procedia*. 140 (2017) 141–150. <https://doi.org/10.1016/j.egypro.2017.11.130>.
- [74] M. Gil-Baez, Á.B. Padura, M.M. Huelva, Passive actions in the building envelope to enhance sustainability of schools in a Mediterranean climate, *Energy*. 167 (2019) 144–158. <https://doi.org/10.1016/j.energy.2018.10.094>.
- [75] I. Ballarini, S. Corgnati, V. Corrado, N. Talá, Improving energy modelling of large building stock through the development of archetype buildings, in: *Build. Simul.*, IBPSA, Sidney, 2011: pp. 14–16.
- [76] J. Kragh, K.B. Wittchen, Development of two Danish building typologies for residential buildings, *Energy Build.* 68 (2014) 79–86. <https://doi.org/10.1016/j.enbuild.2013.04.028>.
- [77] L. Filogamo, G. Peri, G. Rizzo, A. Giaccone, On the classification of large residential buildings stocks by sample typologies for energy planning purposes, *Appl. Energy*. 135 (2014) 825–835. <https://doi.org/10.1016/j.apenergy.2014.04.002>.
- [78] R. Arambula Lara, F. Cappelletti, P. Romagnoni, A. Gasparella, Selection of Representative Buildings through Preliminary Cluster Analysis, in: *Int. High Perform. Build. Conf.*, 2014. <http://docs.lib.purdue.edu/ihpbc/137>.
- [79] E. Liebana, B. Serrano, L. Ortega, Typological analysis of school centres to characterize the energy consumptions . The case of the city of Valencia ., in: *Int. Congr. Sustain. Constr. Eco-Efficient Solut.*, Universidad de Sevilla, Sevilla, 2017: pp. 415–426. <https://idus.us.es/xmlui/handle/11441/59088>.
- [80] S.P. Corgnati, E. Fabrizio, M. Filippi, V. Monetti, Reference buildings for cost optimal analysis: Method of definition and application, *Appl. Energy*. 102 (2013) 983–993. <https://doi.org/10.1016/j.apenergy.2012.06.001>.
- [81] O. Pasichnyi, J. Wallin, O. Kordas, Data-driven building archetypes for urban building energy modelling, *Energy*. 181 (2019) 360–377. <https://doi.org/10.1016/j.energy.2019.04.197>.
- [82] Ministerio de Hacienda, Sede Electrónica del Catastro. Gobierno de España, (n.d.). <https://www1.sedecatastro.gob.es/> (accessed March 2, 2021).
- [83] Municipio del Distrito Metropolitano de Quito, Cédula catastral informativa, (n.d.). https://pam.quito.gob.ec/mdmq_web_cedpredial/procesos/buscarPredio.jsf (accessed March 2, 2021).
- [84] Generalitat de Catalunya, Geoportal del Patrimoni Cultural, (n.d.). <https://sig.gencat.cat/portalsigcultura.html> (accessed March 2, 2021).
- [85] Instituto Nacional de Patrimonio Cultural, Sistema de Información del Patrimonio Cultural Ecuatoriano SIPCE, (n.d.). <http://sipce.patrimoniocultural.gob.ec:8080/IBPWeb/paginas/inicio.jsf> (accessed March 2, 2021).